D4.5

MATERIAL COMPATIBILITY ANALYSIS

Grant Agreement nr	**856998**
Project title	Personalised recovery through a multi-user environment: Virtual Reality for Rehabilitation
Project Acronym	PRIME-VR2
Start day of project (dur.)	January 1st 2023 (3 years)
Document Reference	PRIME-VR2_D_WP4_UOM_D4.5-MCA-v.2
Type of Report	[PU]
Document due date	31/10/2022
Actual date of delivery	30/09/2022
Leader	UOM
Responsible	Emanuel Balzan (emanuel.balzan@um.edu.mt)
Additional main contributors (Name, Partner)	Francesco Tamburrino (francesco.tamburrino@unipi.it) Edward Abela (edward.abela@um.edu.mt)
Document status	[FINAL] (reviewed by EA, GC, PV AR)

This project has received funding from the European Union's Horizon 2020 research and innovation programme under grant agreement N° 856998

This document is shared under the following Creative Commons License

This is a human-readable summary of (and not a substitute for) the license.

You are free to:

Share — copy and redistribute the material in any medium or format

Adapt — remix, transform, and build upon the material

The licensor cannot revoke these freedoms as long as you follow the license terms.

Under the following terms:

Attribution — You must give appropriate credit, provide a link to the license, and indicate if changes were made. You may do so in any reasonable manner, but not in any way that suggests the licensor endorses you or your use.

NonCommercial — You may not use the material for commercial purposes.

ShareAlike — If you remix, transform, or build upon the material, you must distribute your contributions under the same license as the original.

No additional restrictions — You may not apply legal terms or technological measures that legally restrict others from doing anything the license permits.

Notices:

You do not have to comply with the license for elements of the material in the public domain or where your use is permitted by an applicable exception or limitation.

No warranties are given. The license may not give you all of the permissions necessary for your intended use. For example, other rights such as publicity, privacy, or moral rights may limit how you use the material.

Table of contents

List of Figures

List of Tables

EXECUTIVE SUMMARY

Research into additive manufacturing technologies are still in their infancy, although in recent years significant advances have been made particularly in Fused Deposition Modelling (FDM). This project largely exploits FDM printers to manufacture the different components of the controller. However, to produce high-end quality parts – as opposed to prototypes - one must refine the process and toolpath parameters to avoid gross manufacturing defects. Nowadays, advanced FDM printers come with multiple printing nozzles, thus permitting the ability to feed two materials simultaneously, hence multimaterial printing.

Multimaterial printing has opened many possibilities in 3D printing, allowing designers to take advantage of materials' different mechanical properties. Apart from manufacturing two-tone artefacts and possibly two different surface finishes, the objective of multimaterial printing within the PRIME-VR2 project is to achieve local changes in material rigidity across various areas of the bespoke wearable controller.

The most common flexible 3D printing filament available on the market is TPU. On the other hand, different rigid materials such as ABS, PLA and CPE are widely available. The lack of chemical affinity between two materials poses significant challenges to creating functional multimaterial structures. The content being presented in this document stems from the need to investigate and establish compatible 3D printable materials or ways to improve the adhesion strength between two materials at the interface where the two materials meet.

Related literature in this field focuses on finding the ideal material pair, process and toolpath parameters, joint design, or adhesive material to improve the adhesion between two different materials. However, research on the multimaterial is limited. For this reason, this deliverable tests the compatibility of TPU-ToughPLA, TPU-ABS and TPU-CPE+ material pairs with respect to two interface patterns: mechanical interlock and geometric interface.

For this purpose, following tensile testing standards such as ASTM D2095, two different specimens have been created: one has a mechanical interlock interface and the other a geometrical interface. A total of 30 samples, 5 per different material combination and interface pattern, were individually printed using the Ultimaker S5 FDM printer using parameters that the literature recommended. All samples were tested using an Instron 5966 tensile machine which measured the mechanical adhesion strength between the material pair.

Results showed that TPU and PLA have very limited compatibility when a mechanical interlock joint is used compared to the peak forces achieved by TPU-ABS and TPU-CPE+ materials pairs. However, the adhesive strength values measured for geometrical interference samples showed that the adhesion between materials could be increased if a different interface pattern is used. This is clearly evident in cases when tensile testing these samples, for all material pairs, the TPU material failed cohesively before any failure could be observed at the geometrical interference joint.

This document concludes with a number of recommendations that were presented to improve the adhesion between ToughPLA and TPU within the PRIME-VR2 project. Furthermore, potential future research avenues have been identified.

BACKGROUND

This deliverable forms part of the Verification and Validation Testing (VVT) plan, which was added in the project's second year due to the need to have a more profound insight on material compatibility and joint design. As per D4.3, D4.5 falls within stage 1 testing of the proposed VVT strategy.

The study aims to investigate the compatibility of the flexible material TPU (thermoplastic polyurethane) with common rigid materials, namely ToughPLA (Tough Polylactic Acid), ABS (acrylonitrile butadiene styrene), and CPE+ (co-polyester +). Two types of joints will be considered to study whether material compatibility may be improved. The outcome of this study will support future design decisions taken for the controller.

1 INTRODUCTION

Most objects that we used in our daily life are known to be heterogeneous objects (HEOs), that is, made from multiple materials (Yang et al., 2021). Man-made HEOs are typically achieved through a manufacturing process such as multi-material injection moulding, assembly using fasteners or clips, or joinery with an adhesive, fusing or a weld joint, depending on the material(s), production volume requirements and many other criteria. In the last two decades, additive manufacturing (AM) has gained a lot of attention especially because it has revolutionised the way complex-shaped parts are produced. In turn, this has driven research on materials in order to be able to produce personalised parts with the ideally suited characteristics.

The most common consumer level 3D printing technology can produce a fair level of quality parts with great mechanical properties These printers operate via Fused Filament Fabrication (FFF), also known as Fused Deposition Modelling (FDM) or Modelling Extrusion (ME) (Issayev, Aitmaganbet, Shehab, & Ali, 2021; Watschke, Waalkes, Schumacher, & Vietor, 2018). In recent years, such printers have enabled the printing of multiple materials in a single printing process (Harris, Jursik, Rochefort, & Walker, 2019) without the need to apply external adhesive material, thus opening up a myriad of possibilities in the field of product development in various industries, including biomedical, automotive, toy and education. Such technology is not just limited to producing prototype parts or aesthetically pleasing artefacts, but can now also manufacture functional parts with mechanical properties tuned to the required purpose of use.

One of the objectives of the PRIME-VR2 project is to develop a wearable bespoke controller for patients with stroke or musculoskeletal injuries or dystonia, undergoing rehabilitative therapy using VR. To fabricate bespoke devices through well-researched, traditional manufacturing technologies such as injection moulding, it would be economically unfeasible, unless the design is made adjustable to cater for a wide range of users. Still, user variation due to different anthropometrics is wide, and adjustable wearables may result in comfort, user experience, effectiveness or worse, creating further damage. For the controller to be worn and provide an adequate degree of comfort and robustness, it must be composed of flexible and rigid parts. A critical consideration in multimaterial printing is the compatibility between materials, which means that there is good adhesion/bonding between the materials.

Research on the compatibility between low modulus (flexible) and high modulus (rigid) materials has gained traction (Issayev et al., 2021; Tamburrino, Graziosi, & Bordegoni, 2019). This is key in the development of a single multimaterial prints. Even though limitations will always exist due to the material's chemical affinity in binding together, the printing parameters can be adjusted to improve the interlayer adhesion between materials albeit with potential repercussions on the quality of the printed parts (Jiang, Lou, & Hu, 2019). Another way to improve material compatibility is to design better joints or interfaces where the different materials come in contact. These aspects are driven by the theories and mechanisms of adhesion (Nardin & Schultz, 2003).

1.1. Main objective and goal

This deliverable has stemmed from the design requirements of the controller being developed in the PRIME-VR2 project. The use of multi-materials in end-user artefacts manufactured through 3D printing has opened up new design possibilities which allow designers to exploit combinations of different mechanical, chemical and aesthetic properties of materials in functional products. The main goal of this study is to analyse the compatibility between TPU, a low modulus, hence flexible, material with three other typical high-modulus (rigid), thermoplastic materials (Vanaei et al., 2020) used in 3D printing in order to assess the interlayer adhesion strength created through the FDM process. This will provide material and design guidelines on multimaterial prints produced which will be value-adding to the PRIME-VR2 project. Moreover, this research also aims to extend past work of researchers from the

UOP team and the related literature to continue adding knowledge in the field of additive manufacturing.

1.2. Methodology

As depicted in the VVT strategy of Figure 1, this study was driven by the need to investigate the compatibility of 3D printing materials used in the PRIME-VR2. The tests that were carried and documented in this deliverable form part of the first stage of testing where results from testing on materials coupons will be used to support new design work.

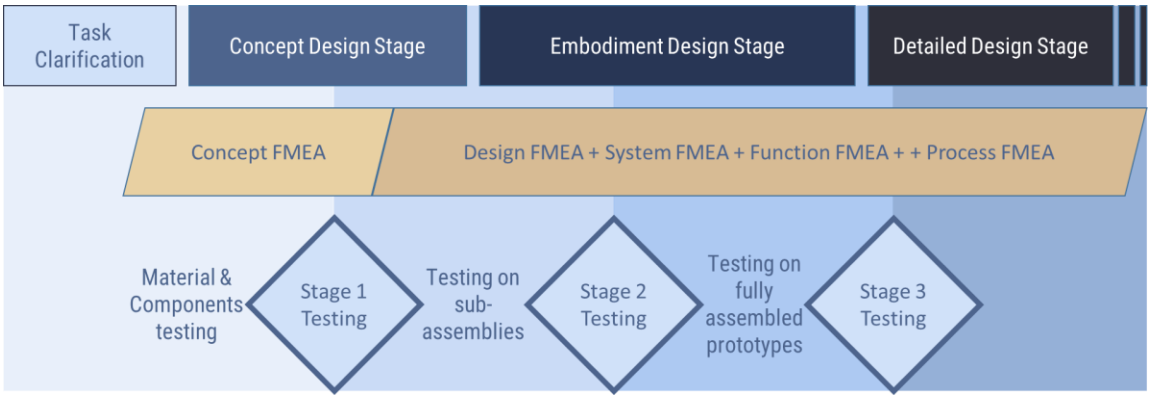

Figure 1:Simplified version of the VVT Strategy adopted by UM in PRIME-VR2

In order to carry a thorough analysis, relevant literature was reviewed. Typical materials used for developing functional prototypes were selected and procured. Based on the findings of (Tamburrino et al., 2019), material coupons were designed, and manufactured. For the tensile test, the method stated in ASTM D2095 (American Society for Testing and Materials. ASTM, 2015) was used. Details about the actual tensile test are listed in Deliverable 4.3 as VVT-04. Table 1 lists the procedure for the tensile testing as outlined in Deliverable 4.3.

Table 1: VVT-04 Material Compatibility, adapted from (Balzan, 2021)

<table>
<tr><td colspan="2">Filing Date: August 2021</td><td>Revision: 0.2</td></tr>
<tr><td colspan="2">Generic VVT activity ID: VVT-04</td><td>Lifecycle Phase: Design</td></tr>
<tr><td colspan="3">Generic VVT activity name: Material Compatibility</td></tr>
<tr><td colspan="3">Specific VVT activity name: Tensile testing of 3D printed material pairs</td></tr>
<tr><td colspan="3">VVT performance level: 0.1
Tensile tests on mechanical interlock and geometric interference specimens involving three materials combinations, namely: TPU-ToughPLA, TPU-ABS, and TPU-CPE+

Type 1: Mechanical Interlock Joint

A mechanical interlocking pattern generated through small wall around the perimeter of the specimen.

Type2: Geometrical Interference Joint

A geometrical interference pattern generated between the 3D models of upper and lower part of the specimen.</td></tr>
<tr><td colspan="3">System/Subsystem: Controller</td></tr>
<tr><td colspan="3">Responsible person: EB
Affiliation: UOM</td></tr>
<tr><td colspan="3">Required equipment/jig/fixture: Instron 5966 testing machine (Bluehill software V4.07)</td></tr>
</table>

Table 1 (cont): VVT-04 Material Compatibility, adapted from (Balzan, 2021)

VVT method: See, ASTM D2095

Test Parameters:

Operating Mode	N/A
Speed of testing	5 ∓10%mm/min
Nominal Strain rate	0.1 mm/min. min
Tensile force	Test to failure (destructive testing)
Specimens	Type 1 and Type 2 samples for each material pair
Number of components under tests	30 (5 of each set, that is, 10 specimens per each material-pair)

1. Procedure for testing:
    a. Place the specimen in the grippers and attach it to the testing machine, taking care to align the long axis of the specimen and the grips with an imaginary line joining the points of attachment of the grips to the machine.
    b. Tighten the grips evenly and firmly to the degree necessary to prevent slippage of the specimen during the test, but not to the point where the specimen would be crushed.
    c. Set the speed of testing at the proper rate as specified in Test parameters table above and start the test.
    d. Record the load at the moment of rupture.

2. Report Results as per standard ASTM D2095:
    a. Complete identification of the material-pair tested, including type, source, manufacturer's code numbers, form, principal dimensions, previous history, etc.,
    b. Method of preparing test specimens,
    c. Type of test specimen and dimensions,
    d. Conditioning procedure used,
    e. Atmospheric conditions in test room,
    f. Number of specimens tested; for anisotropic materials, the number of specimens tested and the direction in which they were tested,
    g. Speed of extension in mm/s,
    h. Tensile strength at yield or break, average value, and standard deviation,
    i. Tensile stress at yield or break, if applicable, average value, and standard deviation,
    j. Percent elongation at yield, or break, or nominal strain at break, or all three, as applicable, average value, and standard deviation,
    k. Modulus of elasticity or secant modulus, average value, and standard deviation,
    l. Date of test, and Revision date of Test Method D638.

Relevant Documents:	ISO 17296-3:2014	ASTM D2095	
VVT activity location:	DMME Lab (UOM)		
VVT activity schedule: From: M33 **To:**M36			
Budget Estimation			
Engineering (hours)		**Cost (K€)** N/A	
System Hours	**VVT Hours**	**Purchasing Cost**	**Subcontract Cost**
Preparation of files: 8hrs Printing: 90hrs	10hrs	N/A	

1.3. Terminology

The following technical terms are used throughout this document. To ensure that the reader understand the meaning of the term as used in this report Table 2 lists their definition.

Table 2: Terminology of terms used

3D	three-dimensional
ABS	Acrylonitrile Butadiene Styrene
Additive manufacturing	*manufacturing process in which material is incrementally added layer by layer*
Chemical affinity	*the tendency of an atom or compound to combine by chemical reaction with atoms or compounds of unlike composition*
Computer Aided Design (CAD)	*the use of computer software to aid in the creation, modification or analysis of a design*
3D CAD model	*a computer 3D model designed/modelled using CAD software*
CPE	*co-polyester*
Drooling effect	*a type of unwanted phenomenon that occurs during 3D printing. It results from the printer heads having the nozzle heated to ensure that when the print head becomes active it starts printing, thus eliminating the wait time for it to heat up. However, as the filament is close to the hotend, it melts and, although it is not being pushed through the nozzle, material starts drooling from the nozzle and may be deposited on unwanted areas. This defect is also known as oozing and stringing.*
Delamination	*a mode of failure where a 3D printed object fractures into layers.*
Elephants footing	*a 3D printing term relating to a wide first layer which can cause unintentional bonding of detailed parts.*
Filament:	*The material which is used during 3D printing (either 1.75mm or 2.85mm)*
Fused Deposition Modelling (FDM) [or FFF printing]	*material extrusion method of additive manufacturing*
Heterogeneous objects (HEO)	*objects made from multiple materials*
Infill Pattern and Infill Density	*the interior of solid volumes in a print can be filled using structures (patterns). The infill density of these structures is controlled by a percentage parameter (0% being hollow, 100% being solid).*
Printer's Bed or Build plate	*the flat, often heated, surface on which the print is constructed*
Process parameters	*refers to the printer settings about the speed and temperature of the printing nozzle*
Slicer Software	*the software used to convert the 3D models to be printed into GCode.*
Toolpath parameters	refers to the printer settings about the layer being deposited.
ToughPLA	*Tough Polylactic Acid is a rigid material widely used filament*

	material for extrusion-based 3D printers
TPU	*Thermoplastic Polyurethane - a flexible material*
Ultimaker S5	*a 3D printer that is manufactured by Ultimaker and uses 2.85mm filament. It is capable of multi-material prints and has a print bed size of 330x240x300mm.*
Virtual Reality (VR)	*Virtual reality is a simulated 3D environment that enables users to explore and interact with a virtual surrounding in a way that approximates reality, as it is perceived through the users' senses.*

1.4. Document Structure

This report is structured as follows. The first section gives an introduction to the study being tackled in this deliverable. Section 2 provides further background to the problem and an account of the state-of-the-art work on the multi-material's adhesion strength. Section 3 outlines the experiment carried out on the test specimens, whereas Section 4 presents the results attained. Some discussion on the results is presented in Section 5 and concluding remarks are drawn in Section 6.

2 PROBLEM BACKGROUND

2.1. Multi-material, extrusion-based 3D printing

FDM is one type of additive manufacturing (AM) process through which 3D complex parts that are impossible or difficult to produce through other manufacturing processes can be fabricated from thermoplastic polymers. As outlined in Section 1 (introduction to multimaterial 3D printing), FDM printers can provide a host of advantages to various users. In the past, FDM's primary purpose was to produce prototype or proof-of-concept, functional or non-functional parts. The first FDM printers were equipped with only one extrusions nozzle, allowing them to create artefacts from a single material. There are many considerations that affect the quality of prints, including the geometry and form of the part, the material's temperature and speed profiles, and environmental conditions (Redwood, Schffer, & Garret, 2017). Such settings influence dimensional accuracy and interlayer adhesion, among others.

The fundamental concept through which a 3D printer works is that material in the form of filament is fed to the printer's head, where a heated nozzle would melt the material and deposit it on the printer's bed (build plate) at a specific rate (speed) and to a specific (x, y and z) position at a specified sequence. The material eventually cools down and solidifies. Once the first layer is printed, the printer's bed moves down so the next layer can be printed. Eventually, the part is formed by printing layer upon layer. This whole 3D printing process is computer controlled. The sequence, speed and position are generated when the slicer software analyses the 3D model to be printed and the material used. One typically finds two nozzles in multi-material FDM printers instead of a single nozzle. Figure 2 depicts an illustration of how a multimaterial printer works.

With the introduction of a second nozzle, FDM printers can now print two objects simultaneously, if equipped with separate printing heads, or handle multimaterial prints, if equipped with a single print head. This advancement also meant new challenges and increased complexity. The deposited material is discontinued during the transition from one nozzle to the other, causing poor mechanical properties or detachment of layers in the printed part (Issayev et al., 2021). As noted in Vanaei et al. (2020) and Yang et al. (2021), extensive research has been carried out to improve the quality of filament materials. However, research on improving the slicing software parameters remains at the forefront in creating strong adhesion between materials.

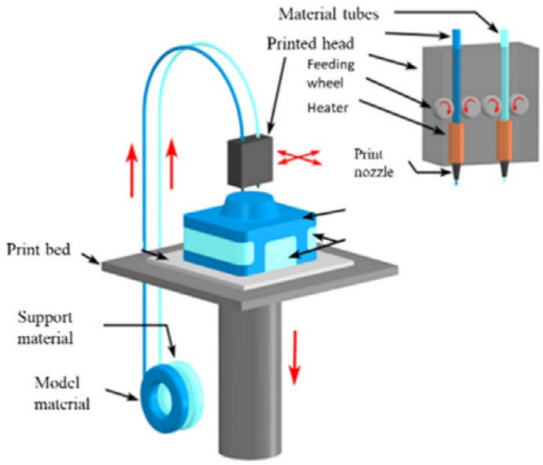

Figure 2: An illustration of how a multimaterial FDM 3D printer works, adopted from (Yang et al., 2021)

Slicing software parameters are divided into toolpath and process parameters (Tamburrino et al., 2019). *Toolpath parameters* include line (deposition) width, layer height (thickness), the gap between the deposited lines, the build orientation (upright, on-edge or flat) and the raster pattern or angle. On the other hand, *process parameters* include extruder feed rate, filament melting or nozzle temperature, the printing environment temperature, build plate temperature and printing speed. Before delving into literature findings, explaining the theory of adhesion is essential.

2.2. Adhesion Strength

Classical theories about adhesion mechanisms are detailed in da Silva, Ochsner, and Adams, (2011); the three which are mostly relevant to FDM are detailed in the next sub-sections. Da Silva et al. (2011) point out that it is essential to distinguish between two types of adhesion: practical and fundamental.

Practical adhesion is related to the force required to break the adhesive bond. This is measured through mechanical testing such as tensile or lap joint testing. This study concerns this type of adhesion. *Fundamental adhesion* is related to molecular forces and mechanisms when two layers are joined together with an adhesive. This type of adhesion is a prerequisite for practical adhesion to take place.

2.2.1. The Mechanical Theory

The theory of adhesion concerns the surface characteristics of the adhesive and the substrate. Figure 3 illustrates how multiple layers are deposited and eventually bonded together on top of each other. Note that the roughness creates voids at the interface between one layer and another.

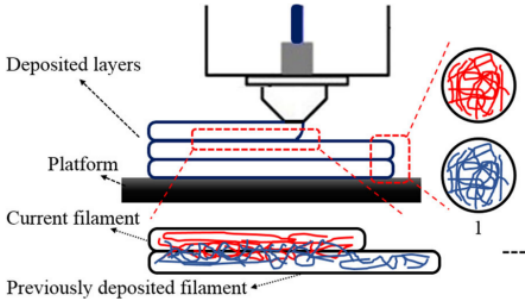

Figure 3: Adhesion of layers, taken from Vanaei et al. (2020)

Mechanical theory states that a rough surface will have higher surface energy than a smooth surface. Tamburrino et al. (2019), explain that if a brittle material is used as the adhesive, the

voids created by the roughness at the interface act as the point of stress concentration, thus lowering the practical adhesion. On the other hand, if a ductile material is used, the stress concentration due to the roughness can enhance the practical adhesion through local plastic deformations. Hence the amount of energy that needs to be dissipated during the failure is higher. Thus, the degree of surface roughness of the two materials influences the practical adhesion.

2.2.2. Absorption theory

Absorption theory states that there will be adhesion whenever two materials come in contact at a molecular level. This theory borrows from the thermodynamic theory, which considers the nature of the contact between the two materials to be very important in establishing strong interatomic and intermolecular forces. This is because the contact angle determines the wettability of a substrate. Therefore, the magnitude of the forces depends on the chemical nature of the surfaces of the two materials, which, in turn, are influenced by the manufacturing process and the design of the interface. If the roughness value of the substrate is not high enough, its effect on wettability is insignificant. Otherwise, if the roughness is high, the wettability of the substrate is reduced, and it negatively affects the joint strength between the substrate and the adhesive (Tamburrino et al., 2019). However, when using a ductile adhesive or material, as in the case of multimaterial printing, practical adhesion can be enhanced due to good wetting with rough surfaces (da Silva, Öchsner, & Adams, 2018).

2.2.3. Diffusion Theory

Diffusion theory is based on the assumption that the adhesion strength of a polymer to itself (autohesion) or another kind of polymer is determined by the extent to which the molecules of the two parts interdiffuse. Optimal adhesion occurs when the interface, that is, the area where one material is in contact with the other, diffuses and does not remain a well-defined as the polymer chains bond together (da Silva et al., 2011; Tamburrino et al., 2019). The dynamics of this adhesion theory are influenced by the temperature, the contact time between the polymers, the contact pressure, their nature (polarity), their molecular weight and the presence of crosslinks. For instance, a high cooling rate causes poor interface bonding.

Da Silva et al. (2011) and Tamburrino et al. (2019) argue that these theories are valid in their individual dimension and must be integrated to fully understand the complexity and the science behind adhesion.

2.3. Related work

Kovan, Altan, and Topal (2017) used the mechanical adhesion theory to study the bonding strength in different printing orientations and specimen thicknesses, as shown in Figure 4. Their results show that for PLA material specimens, the edgewise orientation had the highest layer adhesion strength when it came to smaller layer thicknesses. In contrast, flatwise orientation had the highest bonding strength when the layer thickness increased.

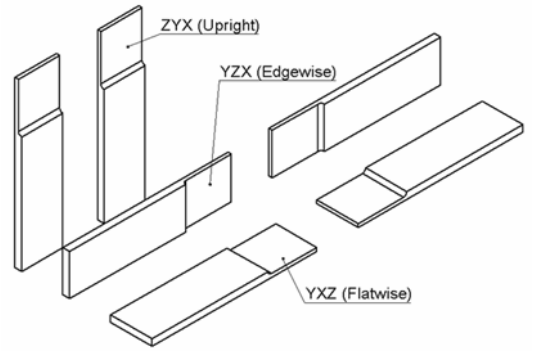

Figure 4: The specimens used in testing different print orientations in Kovan et al. (2017)

The mechanical strength of multi-material bonds made from PLA-TPU and PLA-PTE, among other materials combinations, were investigated by Lopes, Silva, and Carneiro (2018). In this study, multi-section coupons printed in a zebra-crossing structure (see Figure 5) were used, and process parameters were optimised to obtain the maximum strength. Their main findings suggest that both chemical affinity between the materials and the interface (or joint) pattern are essential in increasing mechanical performance.

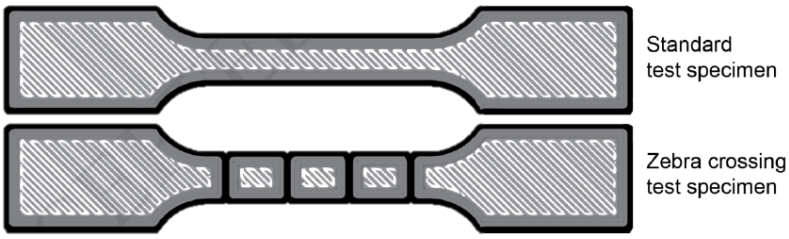

Figure 5: Difference between a standard specimen and a multimaterial, zebra-crossing specimen

In Watschke et al. (2018), tensile, lap-shear and bending tests were carried out according to standard test methods on ABS-PLA material combinations manufactured by FDM. Their study shows that the interface's strength depends on the process parameters and the material properties, such as the glass transition temperature. Low material compatibility between ABS and PLA was reported due to a low interface strength and relatively clean separation.

3D printed parts have a significantly lower strength in the z-direction compared to the strength of parts in the x and y-directions. Vanaei et al. (2020) investigated the effect of temperature on improving the bonding strength (adhesion) between printed layers. They explain that the quality of the bonds depends on the (nozzle) temperature of the current layer being printed — at melting temperature (T_m)— and the temperature of the previously deposited layer. They hypothesised that if the current layer is at T_m and is deposited on a layer at a temperature around crystallisation temperature (T_c), the two layers would bond better because these enable higher material crystallinity. On the other hand, weaker bonds are created if the previously deposited layer temperature is below T_c. During FDM printing, the layers undergo successive cooling and heating cycles. Once the material leaves the extruder, it starts to cool since the environment (and the build plate) are at a lower temperature. Once deposited, the material will transfer heat to the previously deposited layers, which are in the process of cooling, causing them to reheat and ideally surpass T_c. By keeping the previous layer at a temperature slightly higher than T_c, they improve the interlayer bonding strength by 23%.

In (Harris et al., 2019), the multimaterial adhesion strength between TPU and acrylonitrile butadiene styrene (ABS) and TPU with acrylonitrile styrene acrylate (ASA) were investigated. The specimens were shear-tested rather than tensile-tested, and the resultant stress was compared to commercially available adhesives. The results were comparable to such adhesives, suggesting that ASA and ABS are highly compatible and that FDM printing can provide an automated alternative to joints making adhesives. Harris et al. concluded that the lower the viscosity of the material being printed, the higher the strength of adhesion is since low viscosities improve the filling of the interlayer voids.

Tamburrino et al. (2019) investigated the adhesion strength between three pairs of filament materials, namely, TPU-PLA, PLA-CPE, and CPE-TPU, by varying the material printing order, the infill pattern and infill density. In their study, the interface between the two materials was a slightly modified butt-joint, referred to as a mechanical interlock pattern (see Figure 8), to increase the adhesion strength. Their results show that material order and infill density near the interface influence the adhesion strength. They recommend that the rigid material should be printed first and a 100% material infill is to be used near the interface mechanical interlocking pattern. Moreover, they confirmed that mechanical interlocking strategies significantly impact the adhesion strength between materials.

A new multi-nozzle extrusion system for multimaterial FDM printers is proposed in Issayev et al. (2021). The bonding properties between the layers of PLA-ABS, PLA-Flex, and PLA-Flex-ABS material combinations and individual materials were investigated through tensile and compression testing. These researchers concluded that the mechanical properties of the same material with different colours did not change, even if the specimen consisted of two colours. On the other hand, multimaterial printing of different materials resulted in weaker joints, especially for PLA-ABS and PLA-FLEX-ABS material combinations.

In (Khosravani, Soltani, Weinberg, & Reinicke, 2021), the adhesion strength of single-lap joints made from 3D-printed PLA adherents and 0.2mm, 0.43mm and 0.4mm thicknesses of epoxy adhesives, were investigated. The effect of the printing directions for the PLA portions was also investigated. Their results show that such joints are likely to have a cohesive failure (see Figure 6), regardless of the adhesive thickness and the printing parameters of the PLA parts. Moreover, their study revealed that specimens with 0.2mm adhesives provided better structural integrity.

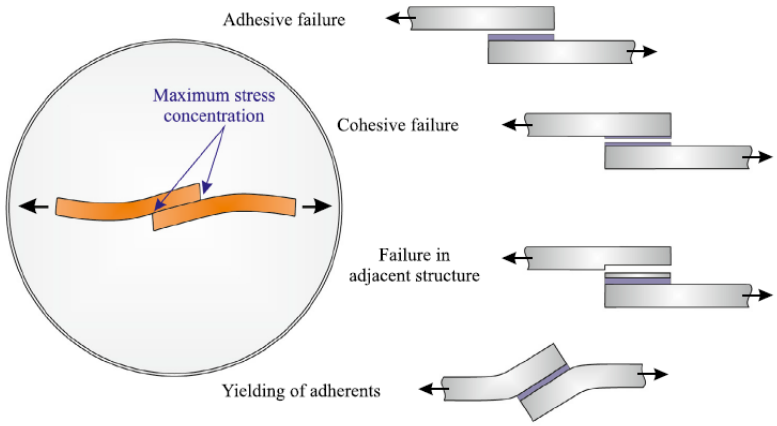

Figure 6: Schematics of different failure modes in adhesively bonded joints, from (Khosravani et al., 2021)

2.4. Concluding remarks on the related work

Research in the field of additive manufacturing and the fabrication of parts using FDM printers is still maturing, as has been shown by the limited amount of published work on adhesion strength within interfaces of multimaterial 3D printed parts. The variation of process and toolpath parameters was found to be effective, but gains in the interface strength can be detrimental to the part quality and dimensional accuracy of the parts. The comprehensive findings of Tamburrino et al. (2019) provide a solid ground for further research of multimaterial components, especially when considering the design of interface patterns. Nonetheless, their study does not thoroughly consider the compatibility of TPU with other commonly used rigid materials.

3 EXPERIMENT

In this section, the materials used, the development of test specimens, and the experimental set-up, are explained.

3.1. Materials

In choosing the suitable material for an artefact, the designer must consider which material characteristics are most critical for the application. The decision is usually based on the application itself, the desired results, the printer's ability to use such materials, the budget, and the available colours.

Different materials are suitable for different applications. For instance, the type of surface texture required or the behaviour required from the parts will determine whether to opt for tough and rigid or lighter and more flexible materials. Printers manufacturers may also sell materials to be used with their printers. This way, manufacturers guarantee material-printer compatibility by specifying what printer settings for optimum part printing quality need to be inputted in the slicer software. Nonetheless, generic materials, that is, materials from different brands, may still be compatible with a specific printer. However, one has to be careful and specify the correct printing settings in the printer's slicing software. Failure to do so, part manufacturing defects such as warping, delamination and elephant's foot are highly probable.

FDM printing material producers offer a wide selection of materials, including sandstone, wood and metal. However, the most common rigid materials are ABS, PLA, PET (PolyEthylene Terephthalate) and Nylon filaments. On the other hand, the most popular flexible filament remains TPU. Filament materials come in a range of tones. Depending on the available colours, the designer may opt for a different material if the mechanical properties are still appropriate for the application. Coloured filaments may influence the cost of the material, but the latter is usually more influenced by the material type.

Based on the requirements for the PRIME-VR2 project and since two Ultimaker (S3 and S5) FDM printers are being used at separate locations by L1D and UOM, it was decided to investigate the adhesion between Ultimaker TPU 95A (Ultimaker, 2022d) (black colour) with three other Ultimaker materials, namely, ToughPLA (Ultimaker, 2022c) (white colour), ABS (Ultimaker, 2022a) (Pearl Gold colour) and CPE+ (Ultimaker, 2022b) (clear colour). Studies of material combinations containing TPU and ABS, ToughPLA or CPE+ have not been conducted. Therefore, apart from investigating the effect of the joint design on the adhesion strength, this study will aim to extend the findings of Tamburrino et al. (2019), thus potentially expanding the library of material combinations available to users.

The following provides a summary of the properties of the selected materials as advertised by the manufacturer, that is, Ultimaker.

3.1.1. TPU

The Ultimaker TPU 95A (Ultimaker, 2022d) is a thermoplastic polyurethane material with a shore hardness of 95A. It is suitable for developing functional, chemical resistant and semi-flexible parts with an overall good consistency. Moreover, the material has strong interlayer bonding. This rubber-like material provides exceptional wear and tear resistance, high impact strength, an elongation of 580% (at break), and good corrosion resistance to many common household industrial oils and chemicals. As the use of TPU with other materials is relatively new to 3D printing, little information is known about its performance when combined.

3.1.2. ToughPLA

The Ultimaker ToughPLA (Ultimaker, 2022c) is similar to its predecessor, PLA (polylactic acid) material, but its toughness is as strong as ABS. Nonetheless, it can be reliably printed with ease, just as PLA, offering the ability to print intricate and fine details. ToughPLA is stiffer than

ABS and less brittle than PLA. Large prints are easier to print than ABS, with fewer chances of warping or delamination. Furthermore, ToughPLA has better post-processing qualities, allowing parts to be sanded for smoother finishes. In contrast, Tough PLA is not suitable for temperatures higher than 60°C.

3.1.3. ABS

Ultimaker ABS (Ultimaker, 2022a) is also one of the most accessible materials for printing functional mechanical parts. It offers excellent interlayer adhesion and good bed adhesion. ABS is suitable for functional properties and fabricating ready-to-use end parts, given its strong material properties. ABS can withstand applications where the temperature does not surpass 85°C.

3.1.4. CPE+

The Ultimaker CPE+ (Ultimaker, 2022b) belongs to the family of CPE (co-polyester) materials, making it chemical resistant, tough, and with good dimensional stability. It is a preferred choice for both functional prototypes and mechanical parts. While both CPE and CPE+ provide similar performance characteristics, CPE+ provides the added benefit of higher temperature resistance (up to 100 ºC) and increased impact strength (10 times tougher). The drawback of CPE+ is that it may suffer from built plate adhesion problems.

Figure 7a to Figure 7d illustrate the different material filaments used for this study.

(a) *(b)*

(c) *(d)*

Figure 7: Ultimaker (a) TPU (black), (b)ToughPLA (white), (c) ABS (pearl gold) and (d) CPE+ (clear) filament material

3.2. Test specimens design

The first aim of the study is to investigate the material compatibility between TPU-ToughPLA, TPU-ABS and TPU-CPE+, when attached through a simple butt-joint. Material pair coupons with this joint are referred to as the *mechanical interlock* samples.

Apart from extending the work of Tamburrino, Graziosi, & Bordegoni (2019) by investigating new pairs of materials, the other aim of the study was to investigate the strength of a multi-layer lap joint created through the 3D printer slicing software when the geometries of two materials interfere with each other. For this reason, the material pair coupons with this joint are referred to as *geometrical interference* samples.

As shown in Figure 8, both specimens have a similar design. However, the joint between the two materials is different, as explained in more detail further on. The coupons were designed as per the standard ASTM D2095-96 for the tensile strength testing of adhesives (American Society for Testing and Materials. ASTM, 2015). The geometry and dimensions of the coupons were modified to address limitations in bonding two materials during multi-material printing. Thus, rather than using specimens with a square cross-sectional area, rectangular specimens were designed to increase the adhesion at the interface between the materials. Overall, the specimen is 90mm long and 13mm wide, made from two different materials, each 45mm long. A right through 6.6mm diameter hole was added to enable fixing of the specimen in the testing jig.

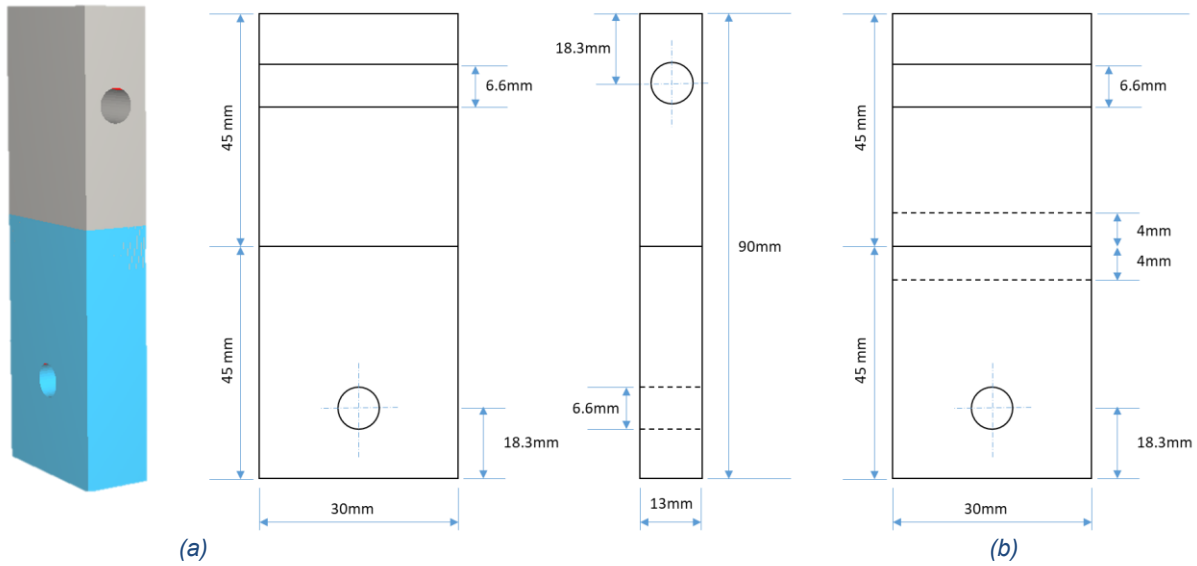

Figure 8: The overall geometry of Type 1 and 2 specimens, adopted from (Tamburrino et al., 2019)

Similar to Tamburrino et al.'s (2019) work, adhesion enhancement techniques, such as plasma treatment and the inclusion of geometric features, were purposefully avoided to investigate the adhesion resulting from the compatibility between the material pairs and the effect of the slicing parameters. The mechanical interlock specimen (Figure 8a) has a small wall around the perimeter of the butt joint. This increases the area of bonded surfaces in the vertical direction, as explained in Section 3.2.1. For the geometric interference specimen, an overlap of 8mm was intentionally created, as shown in Figure 8b. This interference was translated into alternating layers when the 3D model was processed through the slicing software, again as discussed in Section 3.2.2.

To ensure a good sample size, 5 samples were 3D printed using the Ultimaker S5 3D printed and Ultimaker Cura 4.11.0 slicing software for each material-pair and specimen type. This led to thirty specimens being printed: five samples per material combination (three pairs) and joint

designs (two types). Moreover, to ensure that the printing conditions of each sample remain uniform, each sample was printed separately (as shown in Figure 9).

3.2.1. Mechanical Interlock Specimen

The mechanical interlock samples were held in a vertical orientation during printing, as shown in Figure 9. As per the findings of (Tamburrino et al., 2019), for each material combination, it was decided to use TPU for the top material of the specimen (material *B*) since higher adhesion strengths were achieved. This is also because TPU is a deformable material, and printing TPU first will cause an unstable base while printing.

(a) *(b)*

Figure 9: Mechanical Interlock sample viewed (a) virtually in the Cura slicing software, and (b) physically on the Ultimaker S5 printing bed

Printer Settings

A 7mm brim (material *A*) and four ribs (material *B*) were added to material *A* to ensure that the specimen does not detach from the printer bed or warp at the bottom during printing. Both the brim and ribs were removed before tensile testing. Since a layer thickness of 0.3mm was used, each half of the specimen consisted of 150 layers. Figure 10 provides further information on the slicing parameters used.

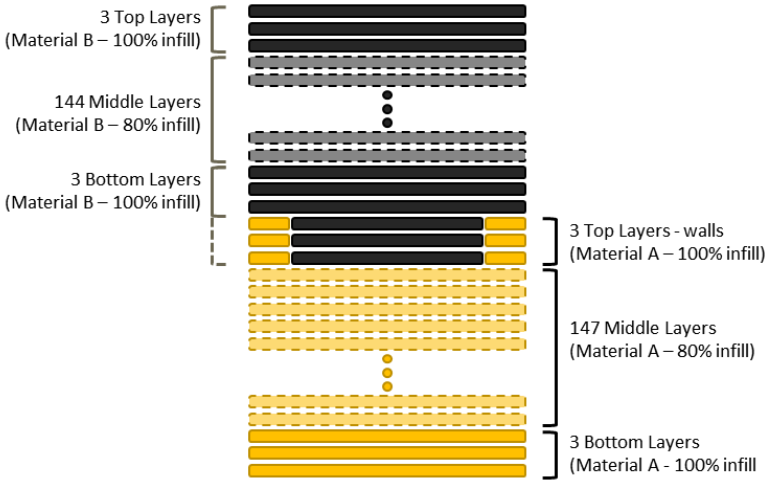

Figure 10: A graphical representation of the printed layers for the Mechanical Interlock specimens

Both material *A* and material *B* consist of 3 clusters of layers: top, bottom and intermediate layers. The top and bottom clusters are made of three layers (0.9mm) and have an infill density of 100%, whereas the intermediate cluster consists of 147 layers (44.1mm) with an infill density of 80%.

The *interface* is the part where material *A* meets material *B*, consisting of the last top layer of material *A* and the first bottom layer of material *B*. In the case of this research study, Material *B* was always the Ultimaker TPU 95A. In Tamburrino et al. (2019), the influence of the material order was investigated and higher tensile forces were identified when the Ultimaker TPU 95A material was at the bottom. The reason why it was opted to have the TPU material at the top for this study was because it was required to investigate the maximum tensile force improvement that could be achieved by changing the interface design, that is, through the geometrical interference.

The infill pattern used for the top, bottom and intermediate layers of both sections was *Lines.* In Tamburrino et al. (2019) it was concluded that the infill pattern does not influence the adhesion force. Figure 11a shows the infill pattern of the print. Note that the direction of the print alternates with each layer. Figure 11b and c show cross-sectional views of the interface.

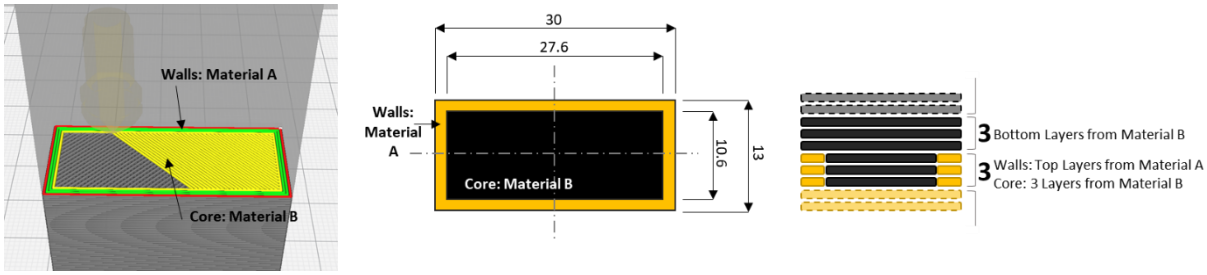

Figure 11: (a) Infill pattern, (b) and (c) show the mechanical interlocking pattern at the interface

As documented in (Carneiro, Silva, & Gomes, 2015), the printing speed influences the adhesion force among the layers because, theoretically, the faster the print, the less time is available for the layer to solidify. Hence layers fuse better. However, Cura's default printing speed values for the different materials were used in different areas of the specimen, as shown in Table 3. This is because higher printing speeds need to be compensated by the percentage flow from the printer's nozzle and would create complications in establishing suitable speeds for the walls, top/bottom layers and travel speeds. It is assumed that the manufacturer has carried out material testing and established the best printing speed parameters for experienced and novice users. Note that the first layer of the bottom cluster of material *A* (which is touching the printing bed) ensures that the coupon remains attached to the bed, and therefore, it is printed thinner and at a lower speed.

Table 3: Printing speeds (mm/s) for the materials used in the study

	Materials Used			
	TPU 95A	ToughPLA	ABS	CPE+
Print Speed	50	50	60	50
Wall Speed	25	36	45	50
Top/Bottom Speed	25	25	350	40
Travel Speed	150	150	150	15
Initial Layer Speed	18	20	10	20

Moreover, the default material printing temperatures and percentage flow was used for all materials, as shown in Table 4.

Table 4: Printing temperatures (°C) and percentage flow for the materials used in the study

	Materials Used			
	TPU 95A	ToughPLA	ABS	CPE+
Print Temperature	225	215	250	270
Plate Temperature	N/A	60	85	110
Flow (%)	106	100	100	100

3.2.2. Geometric Interference Specimen

As shown in Figure 12, the geometric interference samples were held in a horizontal orientation so that the interface, made up of alternating layers, could be printed. Moreover, this figure shows the positions of material *A* and material *B*.

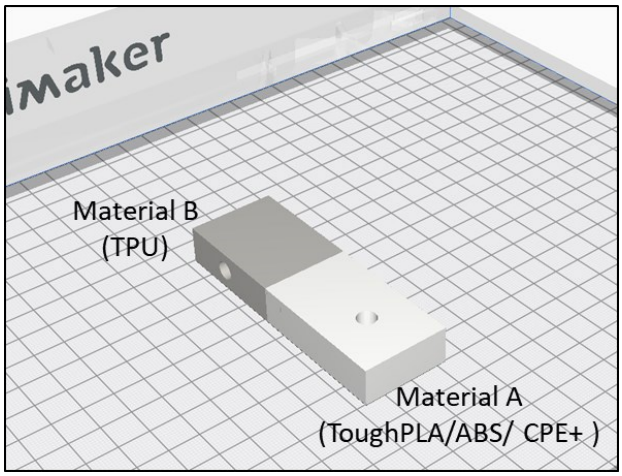

Figure 12: The printing orientation of the Geometric Interference specimen

Printer Settings

Again, a 7mm brim (made from material *A*) was added to the specimen to ensure it does not detach from the printer bed or warp at the bottom during printing. The brim was removed before tensile testing. Since a layer thickness of 0.3mm was used, the specimen comprised 43 layers. A graphical representation of these layers and the infill density is provided in Figure 13 for further information on the slicing parameters used.

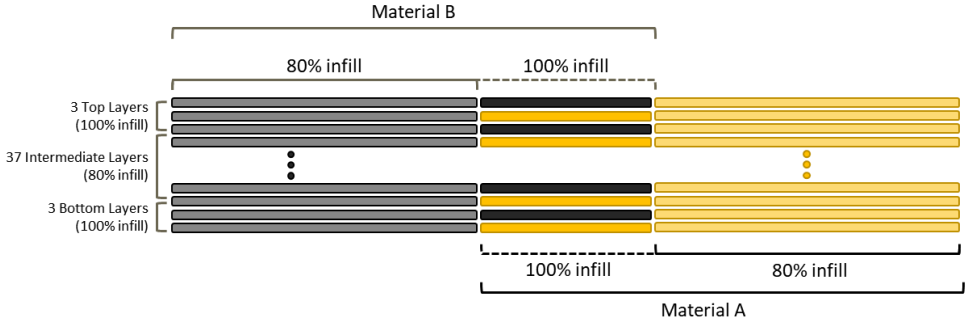

Figure 13: A graphical representation of the printed layers for the Geometric Interference specimens

The top and bottom clusters of layers are made of three layers (0.9mm) and have an infill density of 100%, whereas the intermediate cluster consists of 37 layers (11.1mm) with an infill density of 80%. The *interface* consists of alternating material *A* and *B* layers, as depicted in Figure 13.

The infill pattern used for the top, bottom and intermediate layers of both sections was *Lines* as shown in Figure 14. Note that the direction of the print alternates with each layer as shown in Figure 14.

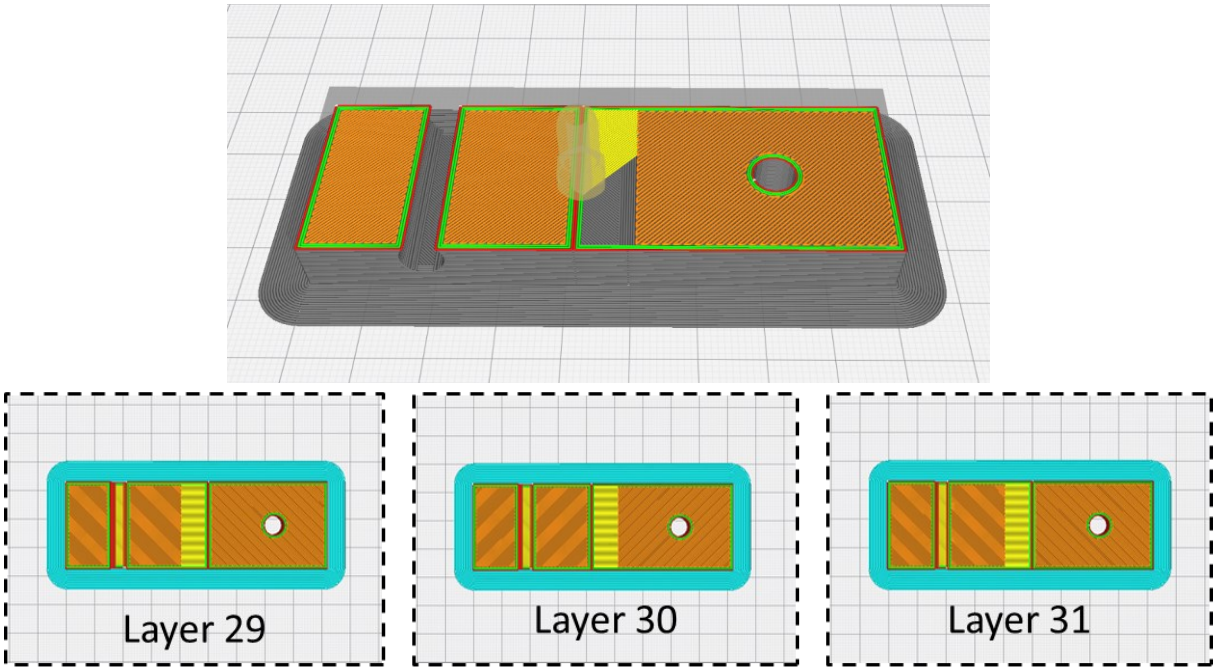

Figure 14: The infill pattern for the Geometric Interference specimen

The same printing speeds and temperatures tabulated in Table 3 and Table 4 were used for the Geometric Interference specimens.

3.2.3. Visual observations on the printed samples

As shown in Figure 15 (a), (b) and (c), five specimens for each material pair were produced for each joint type.

(a) *(b)* *(c)*

Figure 15: Printed Type 1 and Type 2 samples for (a) ToughPLA-TPU, (b) ABS-TPU and (c) CPE+-TPU

A few imperfections were noted both at the interface and along the edges of the specimens. This resulted from uncontrolled drooling/stringing/oozing of TPU material in the other material due to the heated nozzle. Table 5 summarises the number of specimens that contained such

a defect. Figure 16 shows typical, minor imperfections due to the drooling effect at the interface of Type 1 specimens, whilst Figure 17 shows common (TPU) drooling defects along the edges of the specimens. Note that the latter defect does not affect the tensile test, whereas the extent of interface defects was evaluated in the discussion of the results in Section 5.

Table 5: Imperfections

Interface Type	Material Pair	Drooling defects at the interface (# out of 5 samples)	Drooling defects at other areas (# out of 5 samples)
Mechanical Interlock	ToughPLA-TPU	2/5	5/5
	ABS-TPU	5/5	3/5
	CPE+-TPU	2/5	2/5
Geometric Interference	ToughPLA-TPU	0/5	1/5
	ABS-TPU	0/5	2/5
	CPE+-TPU	0/5	3/5

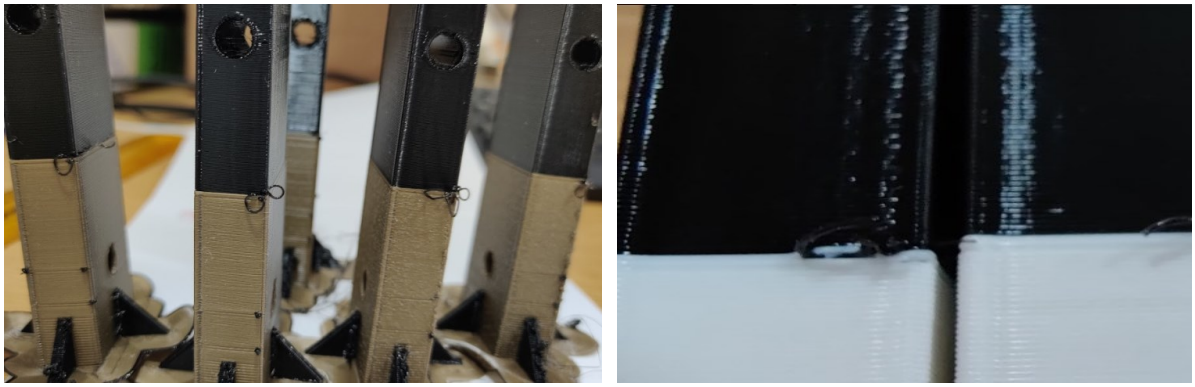

Figure 16:Imperfections due to drooling at the interface of Mechanical Interlock specimens

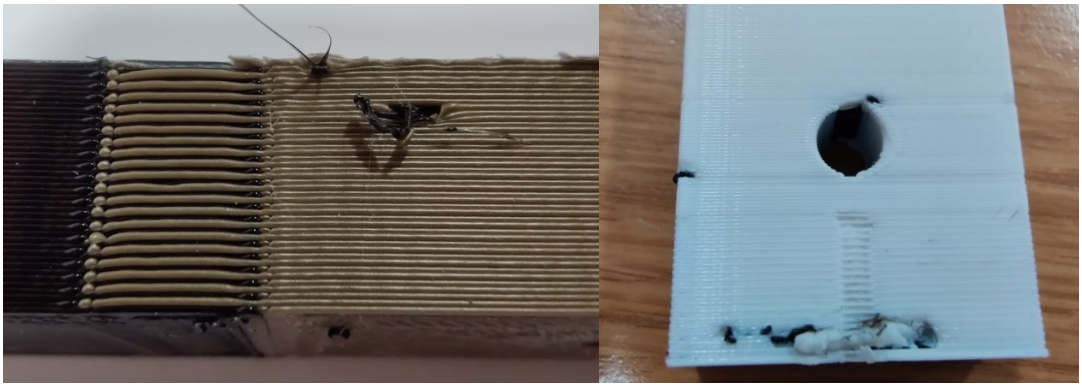

Figure 17: Typical imperfections along the edges of the specimen

3.2.4. Tensile testing machine

The Instron 5966 tensile testing machine shown in Figure 18a was used to measure the 'practical' adhesion of the specimens. The machine is equipped with a 10kN load cell and controlled through Instron's Bluehill software. Custom sample fixtures, shown in Figure 18b, were designed to hold two orthogonal pins and eliminate vertical alignment issues and bending stresses. These grippers were 3D printed from ToughPLA at 100% infill density. The extension rate at the load head was set 5mm/min at a nominal strain rate of 0.1 mm/mm·min was applied.

Moreover, an FLIR E95 thermal imaging camera was used for thermal analysis while testing TPU-ToughPLA specimens. This camera was used to observe any temperature changes

occurring across the sample and particularly at the interface during the test. The outcome of this test and the tensile testing are shown in Section 4 and discussed in Section 5.

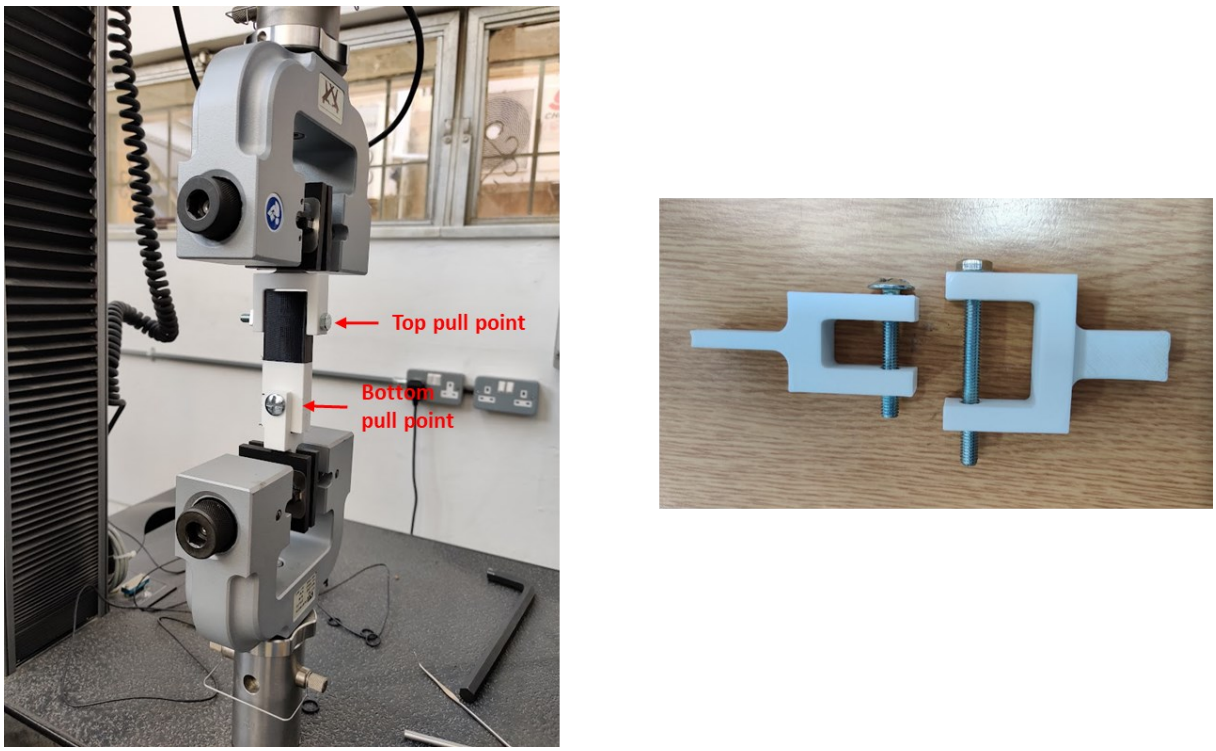

(a) *(b)*

Figure 18: (a) Instron Tensile testing machine, and (b) the grippers used to attach the specimen

4 RESULTS

Tests were carried out on the 6th of June 2022, in a lab with an ambient temperature of 21°C and 60% humidity. The following sections detail the results obtained for the mechanical interlock and geometric interference samples, grouped by material combination. Data outputted by the Instron testing machine was logged into text files. Multiple plots were compiled into ground to allow for comparison of force against displacement. Furthermore, the resultant maximum tensile forces attained were tabulated.

4.1. TPU-ToughPLA

4.1.1. Mechanical interlock samples

Figure 19a and Figure 19b depict a TPU-ToughPLA Mechanical Interlock specimen during tensile testing. The tensile force vs displacement graph for the five samples is shown in Figure 20. This graph shows an amount of variation across specimens. Table 6 lists the maximum forces attained by each sample, the average maximum force and the standard deviation. The average maximum force attained by TPU-ToughPLA mechanical interlock samples is 176N with a standard deviation of 68N.

After the tensile test, the samples' interface was visually inspected for any signs of adhesion failure. As can be seen from Figure 21, the TPU and ToughPLA materials perfectly detach from each other without leaving any residual material on each other, thus indicating a weak joint or compatibility. Although one of the samples' mechanical interlock joint performed weaker than the others, this result implies that minor defects at the joint do not significantly affect the performance of the joint.

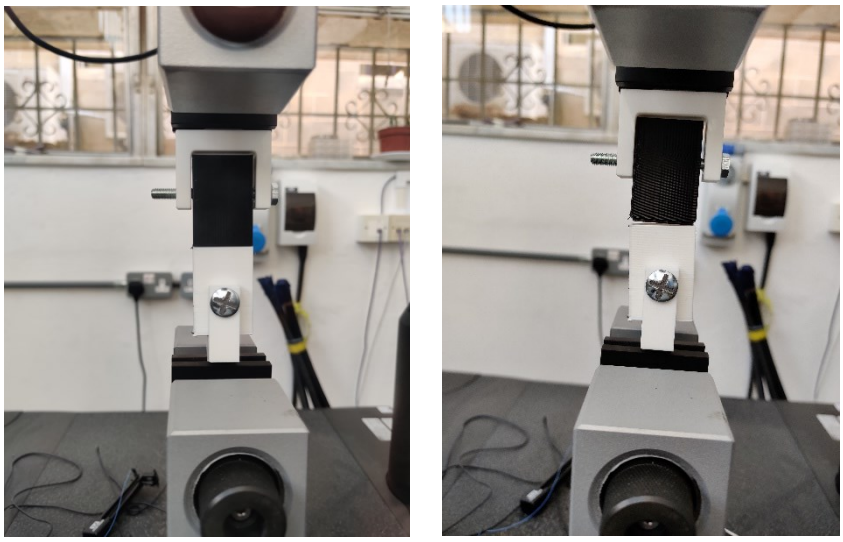

Figure 19: Testing of a TPU-ToughPLA Mechanical Interlock specimen

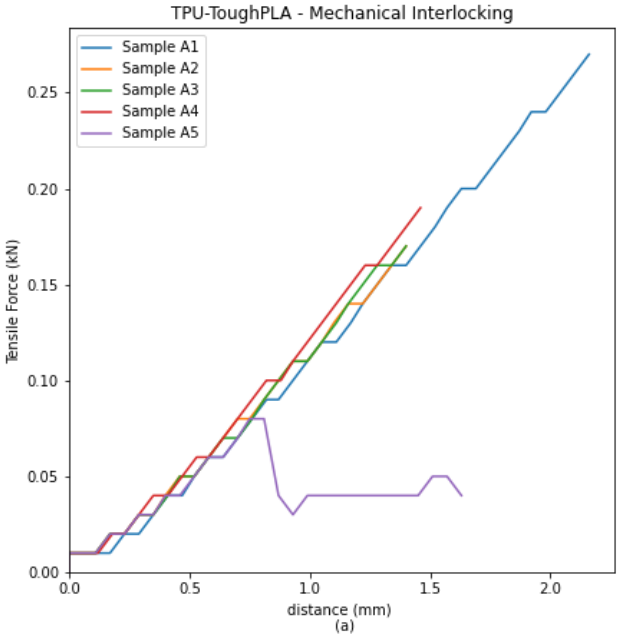

Figure 20: The combined tensile force vs displacement graph of TPU-ToughPLA Mechanical Interlock samples

Table 6: Test data for PLA-ToughPLA mechanical interlock samples

Specimen Number	Maximum Tensile Force (kN)	Average Tensile Force (kN)	Standard Deviation (kN)
Sample A1	0.27		
Sample A2	0.17		
Sample A3	0.17	0.18	0.06
Sample A4	0.19		
Sample A5	0.08		

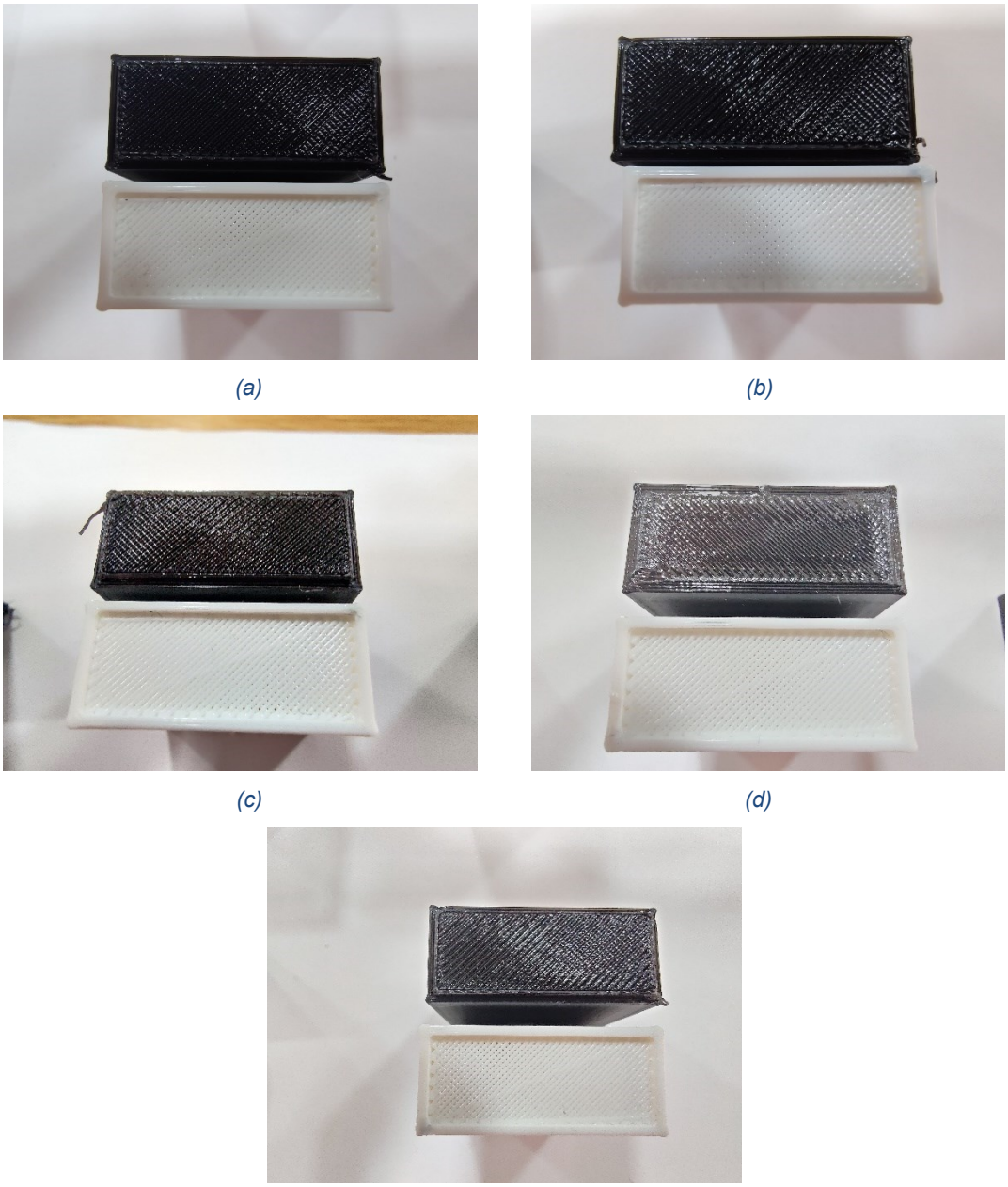

(a) *(b)*

(c) *(d)*

(e)

Figure 21: Close up pictures of the interface of TPU-ToughPLA mechanical interlock samples after tensile test: (a) A1, (b) A2, (c) A3, (d) A4, (e) A5

Figure 22a shows a thermal image of the TPU-ToughPLA mechanical interlock sample during testing (Figure 22b), as regions of a lighter yellow hues can be seen at the top and bottom pulling fixtures. This means that the temperature in those areas was higher. However, moments later, as shown in Figure 22c, higher temperatures were observed near the higher stress regions around the fixture just before the joint failure. A higher temperature was also observed at the interface (joint), meaning that as the joint started to fail, surface energies were higher due to interatomic and intermolecular forces between the two different materials. This can be seen from a measured temperature of approximately 26.2°C in Figure 22a and 28.8°C in Figure 22c. In Bär (2018) this effect is referred to as plasticity induced heating. Note that Figure 22a and Figure 22c are thermal images for the same photo shown in Figure 22b and Figure 22d.

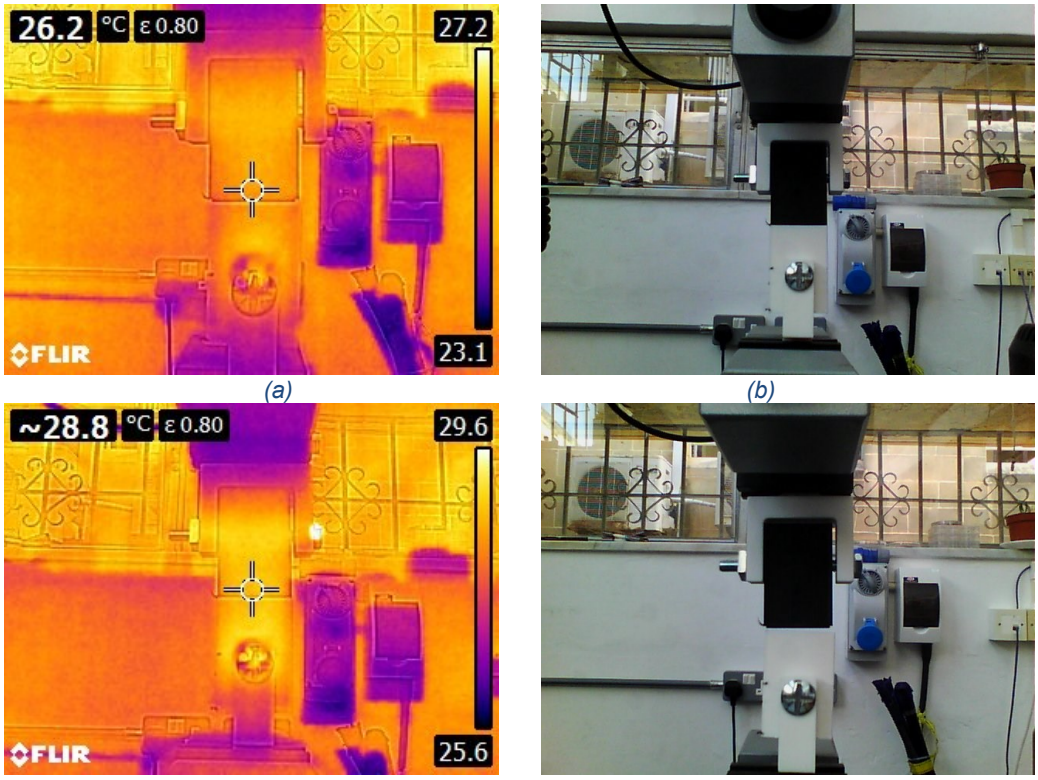

(a) (b)

(c) (d)

Figure 22: Thermal images of a TPU-ToughPLA specimen (a & b) before and (c & d) after testing

4.1.2. Geometrical interference samples

Figure 23a through Figure 23c show a TPU-ToughPLA geometric interference specimen (sample B2) as it was being pulled by the testing machine. As can be seen from these images, the geometrical interference joint did not fail during the test but the TPU material started to experience failure at the TPU section away from the joint and at the pulling fixture. Given its elastic properties, the TPU started to experience cohesive failure, which translated in a drop in the resistance to elongation measured. Samples B3 to B5 did not tear at the joint but at the fixture, whereas the joint of sample B1, as discussed below, started to peel. The combined force-displacement graph for the TPU-ToughPLA specimens in this category is shown in Figure 24. As shown in Table 7, higher tensile forces were obtained when compared to mechanical interlock specimens, as the average maximum tensile force was 1.172kN with a standard deviation of 256N.

(a) (b) (c)

Figure 23: Testing of a TPU-ToughPLA Geometric Interference specimen B2

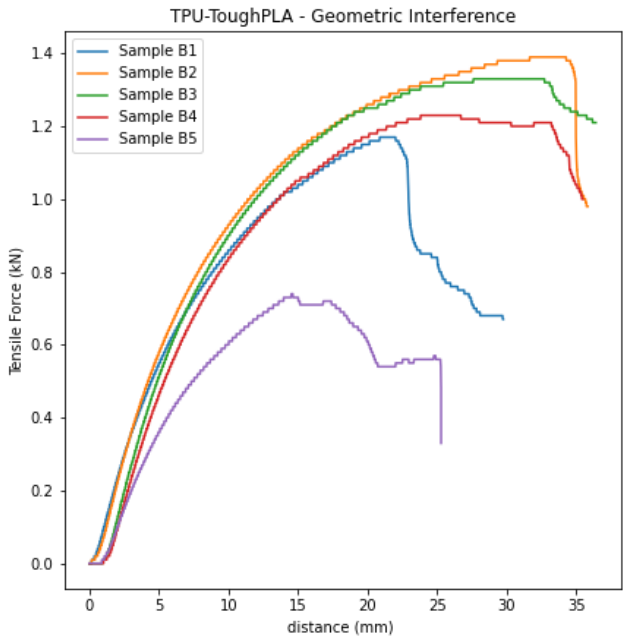

Figure 24: The combined tensile force vs displacement graph of TPU-ToughPLA Geometric Interference samples

Note that sample B5 performed worse than the other samples as the TPU material failed earlier, lowering the overall average maximum tensile force.

Table 7: Basic statistical values for PLA-ToughPLA geometric interference samples

Specimen Number	Maximum Tensile Force (kN)	Average Tensile Force (kN)	Standard Deviation (kN)
Sample B1	1.17		
Sample B2	1.39		
Sample B3	1.33	1.172	0.229
Sample B4	1.23		
Sample B5	0.74		

On closer examination of sample B1, it was noticed that the first and second layers of the specimen started to peel at the geometrical interference joint as shown in the images of Figure 25.

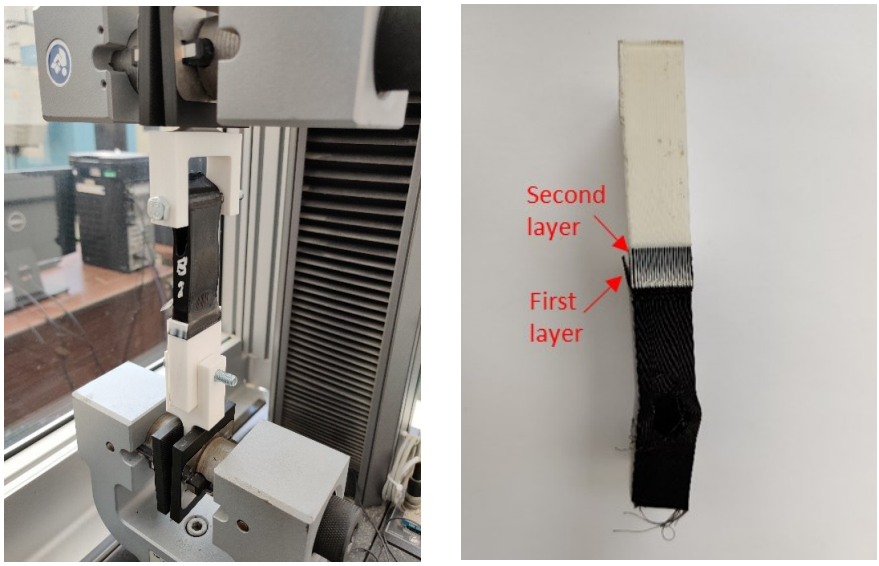

Figure 25: The peeling of the first and second layer of sample B1 at the geometrical interference joint

Thermal imaging on the geometric interference specimens showed higher heat dissipation at the pull points than at the mechanical interlock as an increase of 4-5°C from background environmental temperature level was measured – see Figure 26.

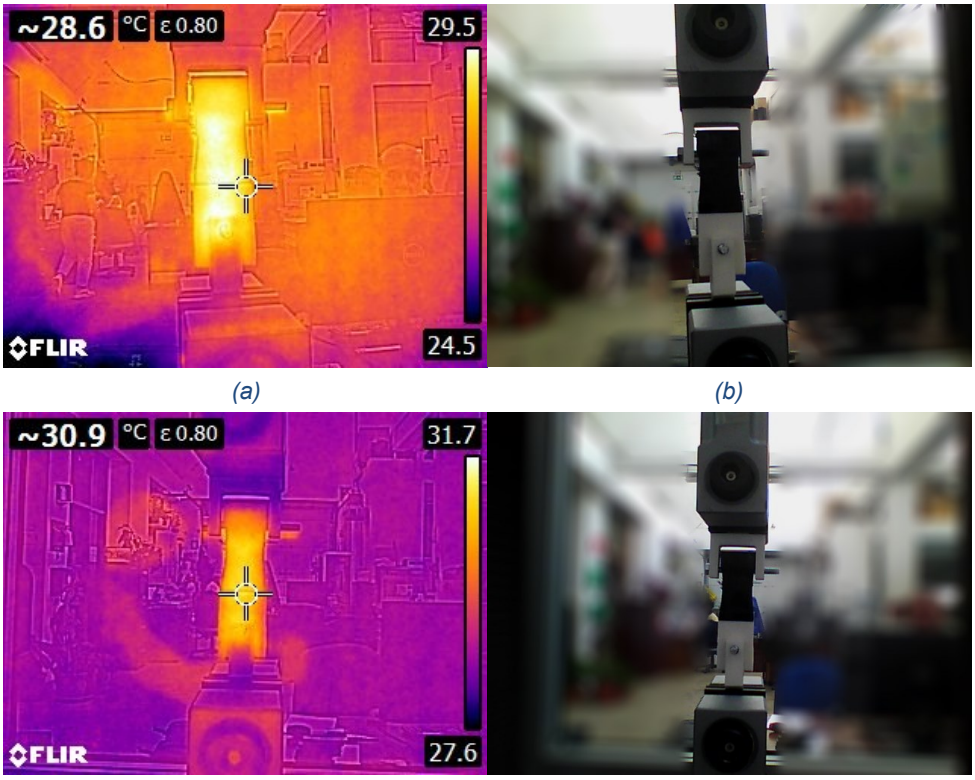

Figure 26: Thermal images of a TPU-ToughPLA geometrical interference specimen during testing: (a & b) at t_1 and (c & d) at t_2

Figure 27 provides a close up view of the tear on the TPU-ToughPLA geometric interference samples at the fixturing anchoring location.

Figure 27: TPU-ToughPLA specimens with geometric interference joint after tensile testing

4.2. TPU-ABS

4.2.1. Mechanical interlock samples

Figure 28 shows a TPU-ABS mechanical interlock specimen while it is being tested. The tensile force vs displacement graph for the five samples in this category is shown in Figure 29. Table 8 lists the maximum forces attained by each sample, the average maximum force and the standard deviation. The average maximum force attained by TPU-ABS mechanical interlock samples is 432N with a standard deviation of 265N. The mechanical interlock joint of samples A3 and A4 failed at lower forces compared to the other samples, causing the average maximum force to be lower and have a larger standard deviation.

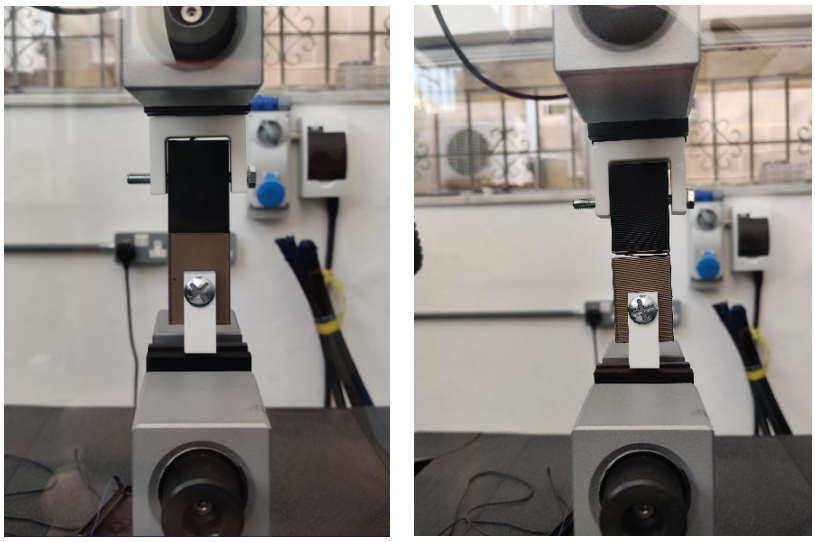

Figure 28: Testing of a TPU-ABS Mechanical Interlock specimen

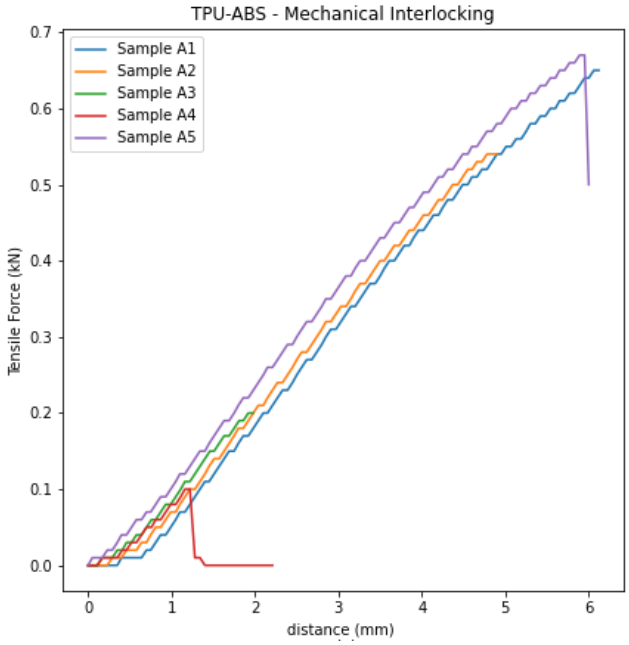

Figure 29: The combined tensile force vs displacement graph of TPU-ABS Mechanical Interlock samples

Table 8: Basic statistical values for PLA-ABS mechanical interlock samples

	Maximum Tensile Force (kN)	Average Tensile Force (kN)	Standard Deviation (kN)
Sample A1	0.65		
Sample A2	0.54		
Sample A3	0.20	0.432	0.237
Sample A4	0.10		
Sample A5	0.67		

After visually inspecting the samples' interface, as seen in Figure 30, the joints of samples A3 and A4 failed without leaving any residual material on each other. This result is similar to the TPU-ToughPLA samples, where the wall of the mechanical interlock and the flat horizontal surface offered little adhesion in the vertical and horizontal directions, respectively. However, in the TPU-ABS combination case, the mechanical interlock wall detached completely, showing better material compatibility.

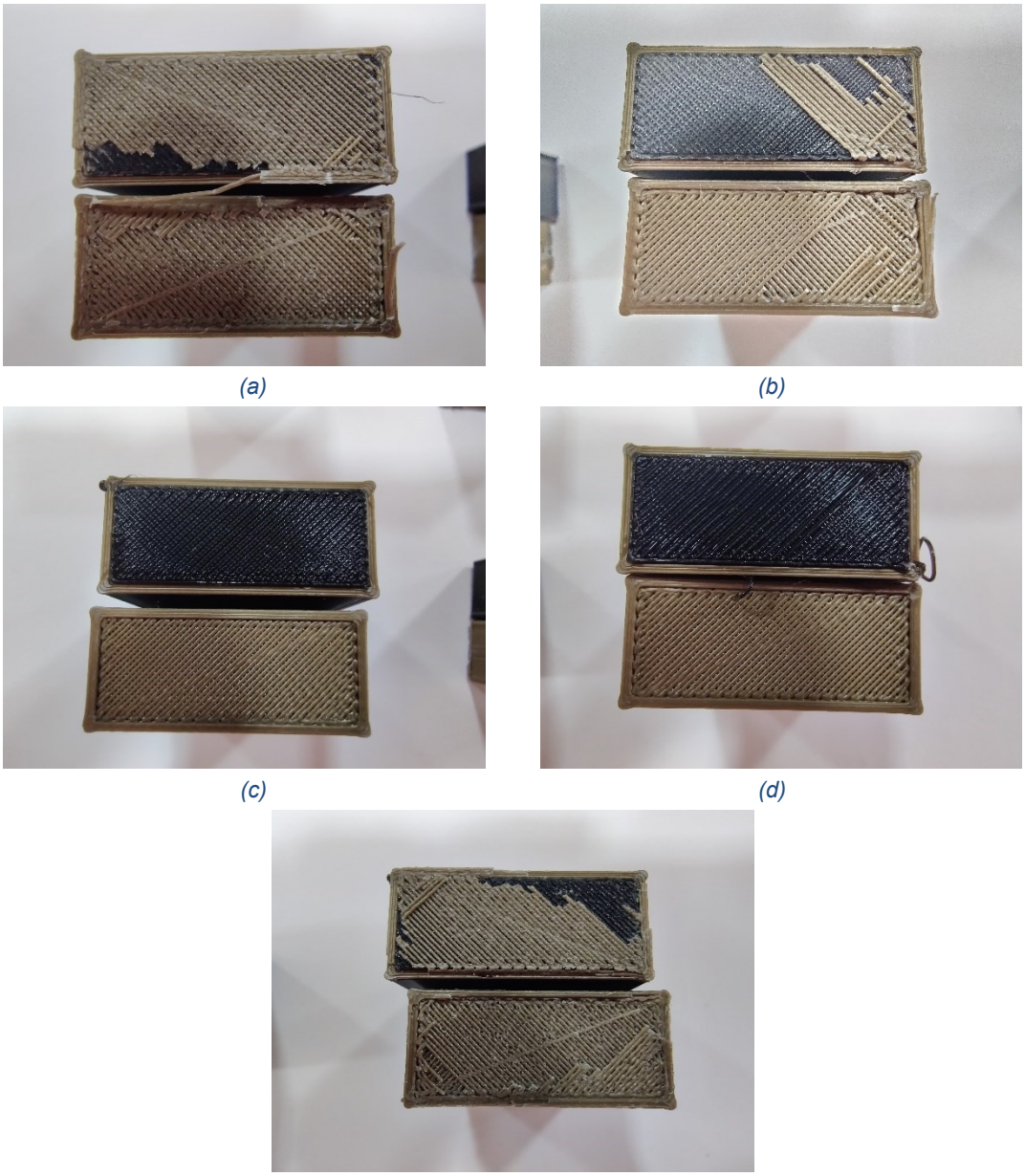

(a) *(b)*

(c) *(d)*

(e)

Figure 30: Close up pictures of the interface of TPU-ABS mechanical interlock samples after tensile test: (a) A1, (b) A2, (c) A3, (d) A4, (e) A5

Figure 31 shows the joint failure of samples A3 and A4 from a different angle. The drooling defect is seen under the wall's second layer.

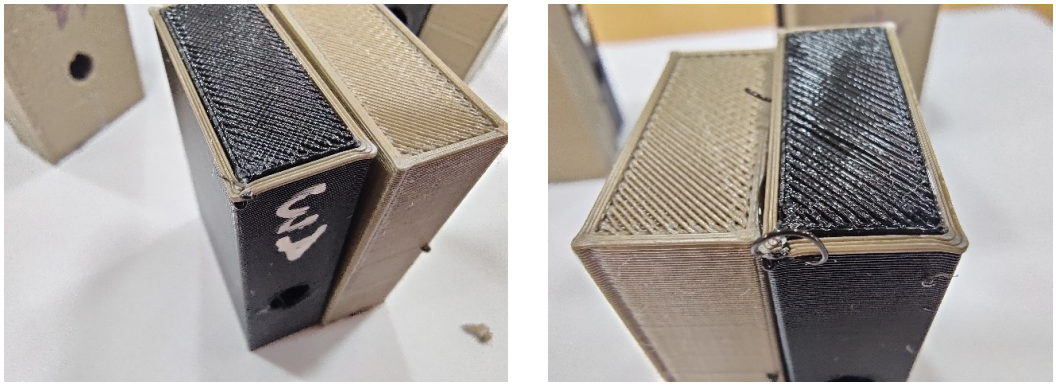

Figure 31: Close up pictures of the imperfection near the mechanical joint of samples A3 and A4

In contrast, samples A1, A2 and A5 show a reasonable degree of compatibility since, after failure, the materials are still partially joined at the failure (see Figure 30). Since prior the test, all samples were seen to have some degree of imperfection at the interface, further testing on newer samples is required. In fact, in sample A1 and A5, the TPU half of the specimens are almost covered in ABS. This was reflected in larger maximum tensile forces.

4.2.2. Geometrical interference samples

Figure 32 shows a TPU-ABS geometric interference specimen as it was being pulled by the testing machine. Similar to the TPU-ToughPLA geometrical interference samples, the specimen did not fail because of a joint failure but because the TPU material started to tear from the top fixture. The combined force-displacement graph for the TPU-ABS specimens in this category is shown in Figure 33.

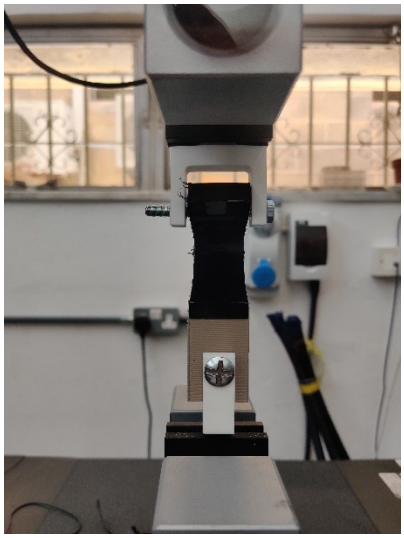

Figure 32: Testing of a TPU-ABS Geometrical Interference specimen

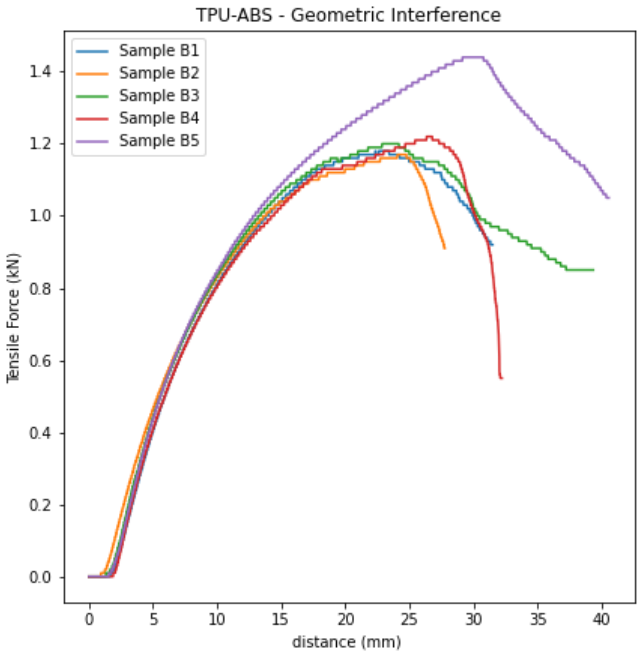

Figure 33: The combined tensile force vs displacement graph of TPU-ABS Geometric Interference samples

As shown in Table 9, similar tensile forces were obtained when compared to the TPU-ABS mechanical interlock specimens since the average maximum tensile force was 1.242kN with a standard deviation of 0.1kN. These values are close to the same specimens made from TPU-ToughPLA since the failure did not occur at the joint but within the material. This indicates that the type of nature of the joint influences the resulting tensile force.

Table 9: Basic statistical values for PLA-ABS geometric interference samples

Specimen Number	Maximum Tensile Force (kN)	Average Tensile Force (kN)	Standard Deviation (kN)
Sample B1	1.18		
Sample B2	1.17		
Sample B3	1.20	1.242	0.100
Sample B4	1.22		
Sample B5	1.44		

Figure 34 provides a close up view of the tear on the TPU-ABS geometric interference samples at the fixture attachment.

Figure 34: TPU-ABS specimens with geometric interference joint after tensile testing

4.3. TPU-CPE+

4.3.1. Mechanical interlock samples

Figure 35 shows a TPU-CPE+ mechanical interlock specimen being tensile tested. The tensile force vs displacement graph for the 5 samples in this category is shown in Figure 36.

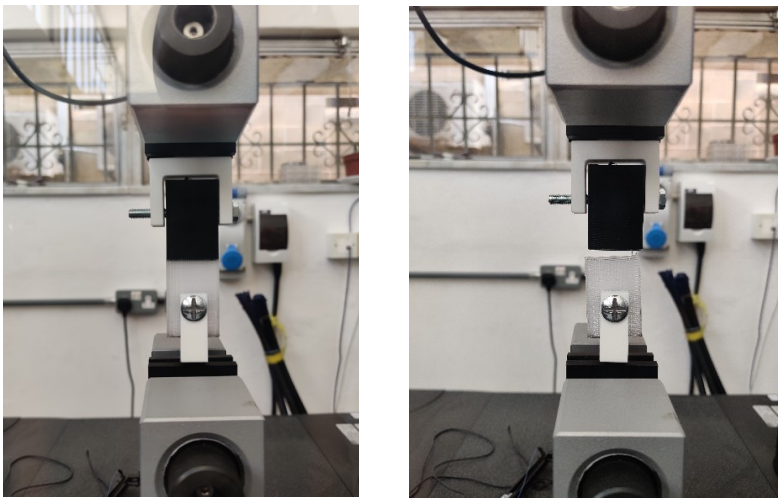

Figure 35: Testing of a TPU-CPE+ Mechanical Interlock specimen

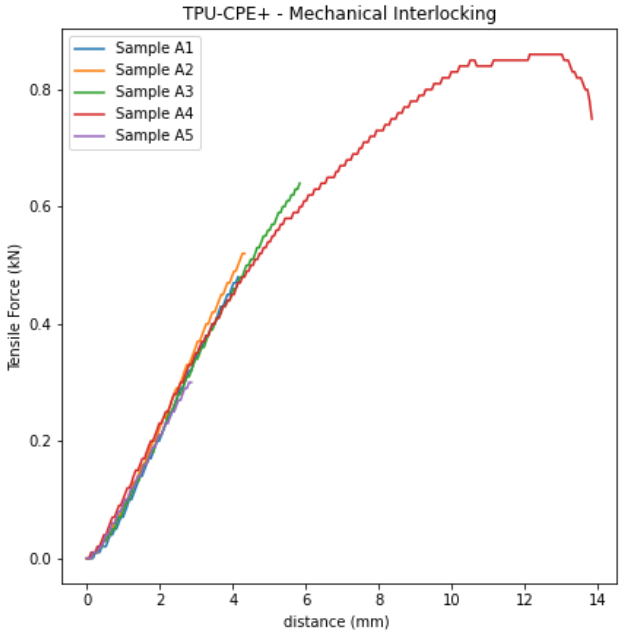

Figure 36: The combined tensile force vs displacement graph of TPU-CPE+ Mechanical Interlock samples

Table 10 lists the maximum forces attained by each sample, the average maximum force and the standard deviation. The average maximum force attained by TPU-CPE+ mechanical interlock samples is 560N with a standard deviation of 207N, indicating better compatibility between TPU and CPE+ than the other pairs. The mechanical interlock joint of sample A5 failed at a relatively lower force, while sample A4 failed at a relatively high force compared to the other samples.

Table 10: Basic statistical values for PLA-CPE+ mechanical interlock samples

Specimen Number	Maximum Tensile Force (kN)	Average Tensile Force (kN)	Standard Deviation (kN)
Sample A1	0.48	0.56	0.185
Sample A2	0.52		
Sample A3	0.64		
Sample A4	0.86		
Sample A5	0.30		

The interface of the broken samples was visually inspected in order to compare the achieved results with the degree of material still attached to the other material. As can be seen from Figure 37, traces of CPE+ detached material were left on the TPU half. Although the extent of the detachment is not as in the TPU-ABS pair, the average force is higher.

From these observations, TPU-CPE+ mechanical interlock samples performed similarly to the TPU-ToughPLA samples since only a few traces of CPE+ can be found on the TPU side. However, contrary to the TPU-ToughPLA samples, none of TPU-CPE+ samples had a clean separation of the mechanical interlock. For instance, two layers from the interlock's vertical walls of samples A1, A2 and A3 are attached with the TPU.

The highest tensile force was obtained by sample A4. As can be seen from Figure 37d, sample A4 left the biggest amount of CPE+ material attached to the TPU at the walls of the mechanical interlock and at the bottom. Compared to the TPU-ABS samples, the TPU-CPE+ material combination seems to less compatible since less TPU surface area is covered by CPE+, even though greater tensile forces were obtained. TPU-ABS performed worse because the adhesion force between ABS layers is weaker than the adhesion force obtained from TPU-ABS layers.

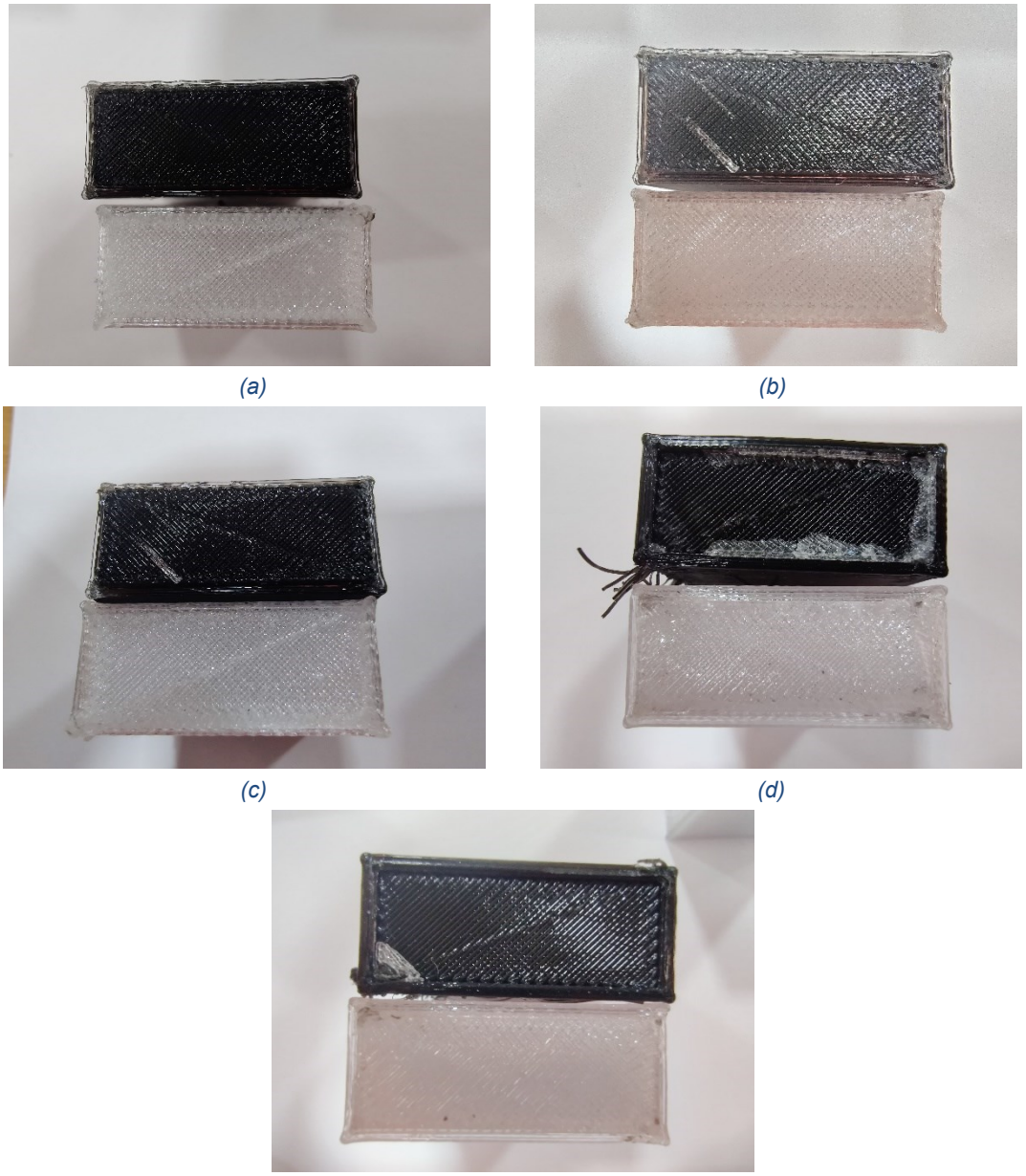

Figure 37: Close up pictures of the interface of TPU-CPE+ mechanical interlock samples after tensile test: (a) A1, (b) A2, (c) A3, (d) A4, (e) A5

On the other hand, sample A5 had the lowest adhesion force and as can be seen from Figure 37 had the cleanest joint after the failure.

4.3.2. Geometrical interference samples

Figure 38 shows a TPU-CPE+ geometric interference specimen as the testing machine ran the extension test. Like the TPU-ToughPLA and TPU-ABS geometrical interference samples, the TPU-CPE+ specimens did not fail because of a joint failure but because the TPU material started tearing from the top holding fixture. The combined force-displacement graph for the TPU-ABS specimens in this category is shown in Figure 39.

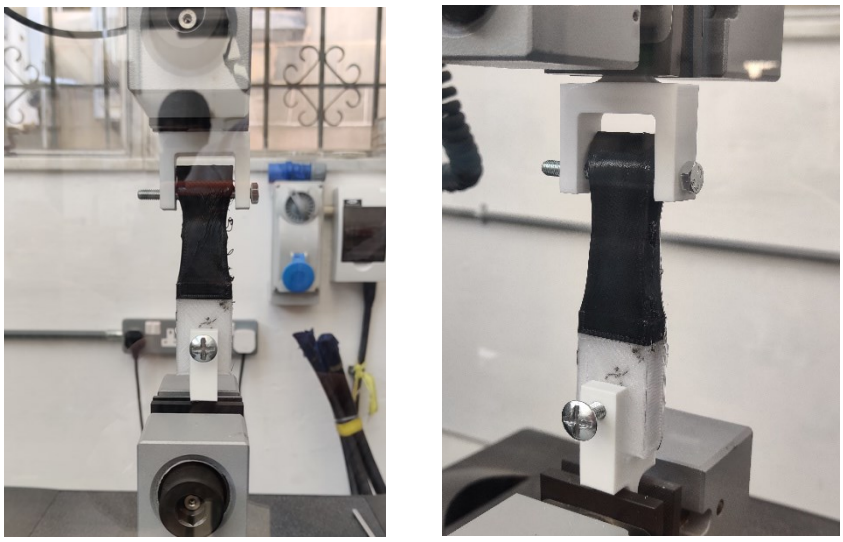

Figure 38: Testing of a TPU-CPE+ Geometric Interference specimen

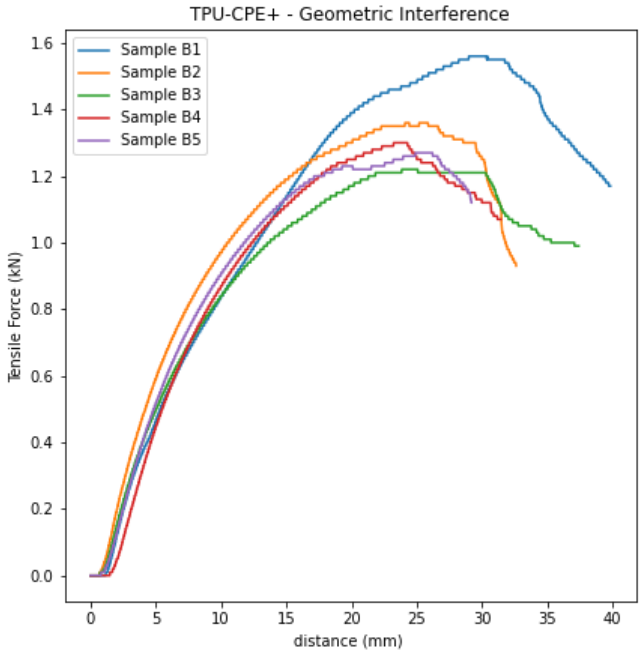

Figure 39: The combined tensile force vs displacement graph of TPU-CPE+ Geometric Interference samples

As shown in Table 11, marginally higher tensile forces were obtained when compared to TPU-ToughPLA and TPU-ABS geometric interference specimens, as the average maximum tensile force was 1.342kN with a standard deviation of 0.118kN.

Table 11: Basic statistical values for PLA-CPE+ geometric interference samples

Specimen Number	Maximum Tensile Force (kN)	Average Tensile Force (kN)	Standard Deviation (kN)
Sample B1	1.56	1.342	0.118
Sample B2	1.36		
Sample B3	1.22		
Sample B4	1.30		
Sample B5	1.27		

Figure 40 provides a close up view of the tear on the TPU-CPE+ geometric interference samples at the pulling point.

Figure 40: TPU-CPE+ specimens with geometric interference joint after tensile testing

5 DISCUSSION

The objective of these tensile tests was to evaluate the practical adhesion of two joint designs between three combinations of materials, namely, TPU-ToughPLA, TPU-ABS, and TPU-CPE+ in order to decide which is the most suitable material pair for the PRIME-VR2 controller. As depicted in Figure 41, higher tensile forces were obtained for the geometrical interference joint compared to the mechanical interlock joint when testing the same material combinations. Sections 5.1 and 5.2 discuss the results in further detail.

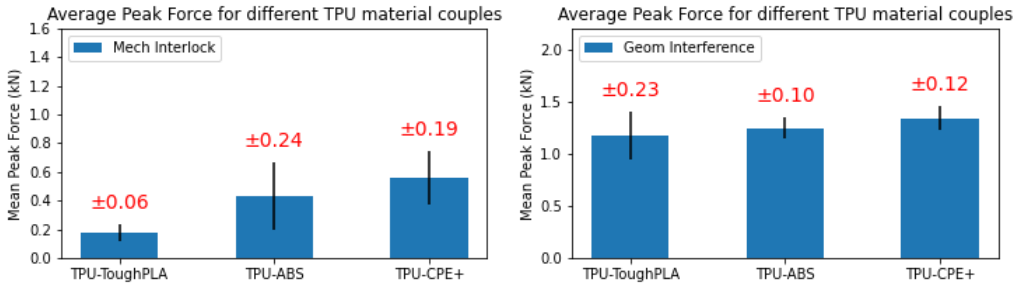

(a) *(b)*

Figure 41: Average peak tensile force for TPU material pairs for (a) mechanical interlock and (b) geometrical interference samples

5.1. Mechanical Interlock Joint

Figure 41a compares the forces the three different material combinations withstood before the mechanical interlock joint failed. These results show TPU and ToughPLA have the least bond strength of the three pairs, with an average load needed to initiate delamination of 176N. This is followed by the TPU-ABS pair at an average adhesion strength of 432N and the TPU-CPE+ combination at 560N. Thus, ABS and CPE+ offer better compatibility with TPU. This could be confirmed from the inspection of the broken mechanical interlock samples in Figure 21, Figure 30 and Figure 37. TPU-ToughPLA pairs show clean top/bottom surfaces at the joint, indicating a weak adhesion.

On this note, it is important to mention that testing of TPU-ABS and TPU-CPE+ material pairs also exhibited instances when failure was characterised by clear cleaved interface surfaces. In turn, these contributed to lower adhesion strengths and lowered the average maximum tensile force of the respective material combination. Manufacturing defects due to drooling (see Section 3.2.3) at the joint might have contributed to such early failures. However, this cannot be affirmed entirely since all five samples of the TPU-ABS combination had the same defect.

In Tamburrino et al. (2019), it was noted that the standard CPE material (similar to CPE+) has already good compatibility due to the diffusion and thermodynamic mechanisms of adhesion. In their study it was reported that compared to the other material combinations (TPU-PLA and PLA-CPE), the design of a simple butt joint does not influence the adhesion strength of TPU-CPE. This may be caused by the higher printing temperature of CPE, and since it is printed first, it bonds better with TPU. An average peak stress of 0.94MPa was reported for TPU-CPE mechanical interlock samples. Peak stress is calculated by dividing the maximum force by the area in contact. Assuming that the area of surface in contact, that is, including the area of the vertical walls, was computed in the same way (see Figure 42), the peak stress translates into a maximum force of 431N). In case the wall surface area was not considered but the cross-sectional area of the specimen, the actual maximum force is 366.6N.

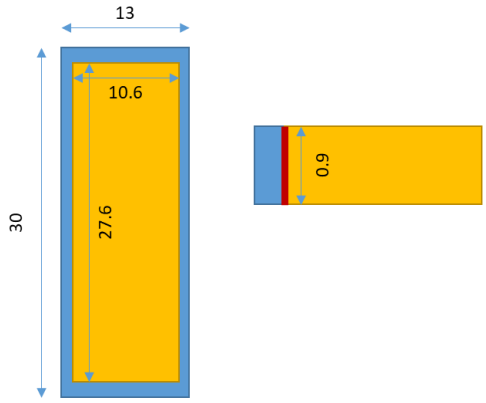

Total Area = specimen cross-sectional area
+
area of walls
= 30*13 + 2*0.9*(27.6+10.6)
= 390 + 68.76
= 458.76mm^2
= 0.00045876m^2

Figure 42: Area of the surfaces in contact

Table 12 lists the average peak stress of the considered material pairs.

Table 12: Average peak stresses experienced by the geometric interference samples

Material Pair	Peak Stress (MPa)
TPU-ToughPLA	0.45
TPU-ABS	1.11
TPU-CPE+	1.44

This study found that using CPE+ instead of CPE can improve the adhesion strength by at least an average force of 129N. It is important to note that CPE+ is printed at a temperature 20°C higher than that of CPE (and 45°C higher than TPU).

Between the ABS and CPE+ material combinations, excluding the samples that had a clean interface after separation, ABS seems to have better compatibility with TPU, given that a larger surface area of ABS remained attached to the TPU. TPU-ABS samples may have separated at a lower tensile force because of manufacturing defects at the interface. For this reason, further experiments are necessary to determine this hypothesis.

As such in conclusion, the material pair with the highest compatibility is TPU-CPE+, closely followed by TPU-ABS and then TPU-ToughPLA.

With regard to the thermal analysis during testing, it can be said that at the site of attachment to the fixture, the temperature is higher due to the amount of stress generated from the holding pins. A relatively smaller hot spot at the interface of the mechanical interlock was also noticed just before the sample failed as the layers separated.

5.2. Geometrical Interference Joint

Figure 41b compares the forces that the three different material combinations withstood before the TPU material failed when the specimens had a geometrical interference joint. These results provided further insight on the adhesion strength between different materials, specifically that, it is not just about the printer settings and the innate chemical affinity between the material combinations but also due to the design of the joint. Through these samples, it was shown that a multi-layered joint could significantly increase the strength of a joint. The actual compatibility between the materials remained the same, but the multi-lap joint design in the direction of the pulling force has decreased the shear stress on the joint by adding a significant resistance to delamination. This is further explained below in Figure 43.

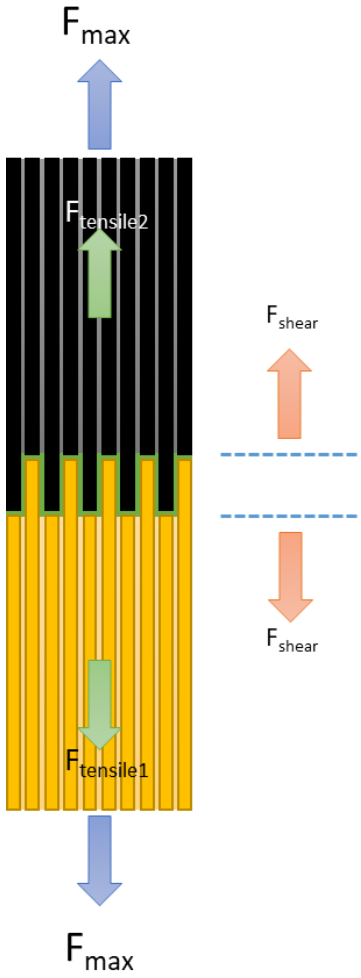

Figure 43: Forces acting on the geometrical interference specimen

The geometric interference specimen can be regarded as composed of three segments, as shown in Figure 43. F_{max} is the gross force being exerted on the specimen to effect failure. Note that F_{max} is not the sum of $F_{tensile}$ and F_{shear} since the gross force is only being translated through the system. F_{max} is translated to tension in the different materials, i.e. $F_{tensile1}$ and $F_{tensile2}$. This is then entirely translated to shear force in the middle segment composed of various multi-lap laminates. In other words, F_{max} is translated into $F_{tensile}$ within the material, which is then directly translated into F_{shear}, acting as a sum of the multiple laminates interlocking each other. Hence if the shear force within the interlock is strong enough between the two materials then the specimen will fail in tension at other areas of the material, such as at the interlock boundary (as seen by sample B2 of the TPU-ToughPLA pair) or at the gripper (as seen by all the other samples). In such a case the material starts to tear.

On the other hand, if the F_{shear} between laminates is weaker than the $F_{tensile}$ being applied, then the layers will start to slide apart (as started to happen to sample B1 of the TPU-ToughPLA pair).

Since all of the geometric interference samples experience a tear at the pulling point or after the joint, it can be assumed that the peak or gross force equivalent to F_{max} directly affects the peak stress within the system. Given that the geometric interference joint, also referred to as the multi-lap joint, remained intact, it is considered as one system and thus, F/A applies also to determine the maximum stresses ($F_{tensile}$) within the laminates just before the material delaminated. Thus, for an area of 0.00039m^2 the average peak stresses experienced at the joint by the different material pairs considered in this study are listed in Table 13. Note, Table 13 does not show the maximum stress withstood by the joint.

Table 13: Average peak stresses experienced by the geometric interference samples

Material Pair	Peak Stress (MPa)
TPU-ToughPLA	3.01
TPU-ABS	3.18
TPU-CPE+	3.44

Comparing the average peak stresses of the mechanical interlock and geometric interference it can be said that the geometrical interference joint has significantly increased the bond between the two corresponding materials.

6 CONCLUSION

Multimaterial printing offers a host of possibilities in the field of artefact design, some of which are considered for aesthetical purpose only due to weak layer adhesion between the different materials. This results either from poor material compatibility, printing settings and conditions, or the design of the joint between the materials. This study investigated the latter aspect of multimaterial printing in order to establish suitable materials for the PRIME-VR2 controller.

The results show that the type of joint used within a multimaterial print heavily influences the adhesion strength between materials. Mechanical interlock joints are weaker than the geometric interference joints especially for the TPU-ToughPLA material pair which requires a low tensile force to separate the two materials. Compared to the other two material combinations considered in this study, the TPU ToughPLA materials are practically incompatible with each other. This renders the ToughPLA material a less suitable candidate within the PRIME-VR2 project given that TPU-ABS and TPU-CPE+ offer a tensile force that is 100% to 200% that of TPU-ToughPLA, respectively.

However, when a geometrical interference joint, consisting of a 42-layers lap joint, is considered, the tensile properties of the joint are stronger than the pull point feature within the TPU material, and irrespective of the material combination used, the joint survives the tensile test. Thus, to guarantee strong adhesion, the TPU material should be interlaced with the other material, especially in thick sections.

These results call for further studies in the field of joint design for multimaterial printing to investigate their affect in different axes of the object, especially since this type of joint can only be printed in one orientation. Other research avenues that are worth investigating are the number of lap joints and the area of the interface may be explored further to find a compromise on the thickness of the joint. This research did not investigate the effect of colorants within materials but as based on the findings of (Issayev et al., 2021) it was assumed that the material colours does not influence the tensile strength.

In product design, the materials are selected based on their properties and the application they will be used for. ToughPLA has an impact strength similar to that of ABS but a higher stiffness. It has excellent surface finish and more reliable than ABS in 3D printing, meaning less defects. On the other hand, CPE+ has high chemical resistance and is resistant to high temperatures up to 100°C. ToughPLA is resistant up to 60°C temperatures, meaning that for the application of the PRIME-VR2, the material can be used.

Another aspect that one considers is the price of the material. ToughPLA is more than 26% cheaper that CPE+ and 5% more expensive than ABS. However, ABS is more technical challenging to print. Moreover, ABS and CPE+ require a higher printing temperature (250°C and 270°C) compared to TPU (215°C), making artefacts made from TPU cheaper to produce due to lower power consumption.

7 REFERENCES

American Society for Testing and Materials. ASTM. *D2095-96 Standard Test Method for Tensile Strength of Adhesives by Means of Bar and Rod*. , (2015).

Balzan, E. (2021). *D4.3 - A Comprehensive Verification, Validation and Testing Plan for the PRIMVE-VR2 Controller Devices*. Malta.

Bär, J. (2018). Plasticity induced heating-an underestimated effect in monotonic and cyclic deformation? *Procedia Structural Integrity*, *13*, 947–952. https://doi.org/10.1016/j.prostr.2018.12.177

Carneiro, O. S., Silva, A. F., & Gomes, R. (2015). Fused deposition modeling with polypropylene. *Materials and Design*, *83*, 768–776. https://doi.org/10.1016/j.matdes.2015.06.053

da Silva, L. F. M., Ochsner, A., & Adams, R. D. (2011). Handbook of Adhesion Technology. In *Handbook of Adhesion Technology: Second Edition* (Vol. 1–2). https://doi.org/10.1007/978-3-319-55411-2_22

da Silva, L. F. M., Öchsner, A., & Adams, R. D. (2018). Handbook of Adhesion Technology: Second Edition. In *Handbook of Adhesion Technology: Second Edition* (Vol. 1–2). https://doi.org/10.1007/978-3-319-55411-2

Harris, C. G., Jursik, N. J. S., Rochefort, W. E., & Walker, T. W. (2019). Additive Manufacturing With Soft TPU – Adhesion Strength in Multimaterial Flexible Joints. *Frontiers in Mechanical Engineering*, *5*(July), 1–6. https://doi.org/10.3389/fmech.2019.00037

Issayev, G., Aitmaganbet, A., Shehab, E., & Ali, M. H. (2021). Bonding Strength Analysis of Multi-material and Multi-color Specimens Printed with Multi-extrusion Printer. *Manufacturing Technology*, *21*(5), 627–633. https://doi.org/10.21062/mft.2021.072

Jiang, J., Lou, J., & Hu, G. (2019). Effect of support on printed properties in fused deposition modelling processes. *Virtual and Physical Prototyping*, *14*(4), 308–315. https://doi.org/10.1080/17452759.2019.1568835

Khosravani, M. R., Soltani, P., Weinberg, K., & Reinicke, T. (2021). Structural integrity of adhesively bonded 3D-printed joints. *Polymer Testing*, *100*. https://doi.org/10.1016/j.polymertesting.2021.107262

Kovan, V., Altan, G., & Topal, E. S. (2017). Effect of layer thickness and print orientation on

strength of 3D printed and adhesively bonded single lap joints. *Journal of Mechanical Science and Technology*, *31*(5), 2197–2201. https://doi.org/10.1007/s12206-017-0415-7

Lopes, L. R., Silva, A. F., & Carneiro, O. S. (2018). Multi-material 3D printing: The relevance of materials affinity on the boundary interface performance. *Additive Manufacturing*, *23*, 45–52. https://doi.org/10.1016/j.addma.2018.06.027

Nardin, M., & Schultz, J. (2003). Theories and Mechanisms of Adhesion. In *Handbook of Adhesive Technology, Revised and Expanded*. https://doi.org/10.1201/9780203912225.pt2

Redwood, B., Schffer, F., & Garret, B. (2017). *The 3D Printing Handbook: Technologies, Design and Applications* (1st ed.).

Tamburrino, F., Graziosi, S., & Bordegoni, M. (2019). The influence of slicing parameters on the multi-material adhesion mechanisms of FDM printed parts: an exploratory study. *Virtual and Physical Prototyping*, *14*(4), 316–332. https://doi.org/10.1080/17452759.2019.1607758

Ultimaker. (2022a). *ABS*.

Ultimaker. (2022b). *CPE+ Technical Data Sheet*.

Ultimaker. (2022c). *Tough PLA Technical Data Sheet*.

Ultimaker. (2022d). *TPU 95A Technical Data Sheet*.

Vanaei, H. R., Raissi, K., Deligant, M., Shirinbayan, M., Fitoussi, J., Khelladi, S., & Tcharkhtchi, A. (2020). Toward the understanding of temperature effect on bonding strength, dimensions and geometry of 3D-printed parts. *Journal of Materials Science*, *55*(29), 14677–14689. https://doi.org/10.1007/s10853-020-05057-9

Watschke, H., Waalkes, L., Schumacher, C., & Vietor, T. (2018). Development of novel test specimens for characterization of multi-material parts manufactured by material extrusion. *Applied Sciences (Switzerland)*, *8*(8). https://doi.org/10.3390/app8081220

Yang, J., Li, N., Shi, J., Tang, W., Zhang, G., & Zhang, F. (2021). *Multimaterial 3D Printing Technology*. Academic Press, Elsevier Ltd.